

1 **RESEARCH ARTICLE**

2

3 **The *Arabidopsis* MOS4-associated Complex Promotes**
4 **MicroRNA Biogenesis and Precursor Messenger RNA Splicing**

5

6 **Tianran Jia^a, Bailong Zhang^a, Chenjiang You^{a,b}, Yong Zhang^a, Liping Zeng^a,**
7 **Shengjun Li^c, Kaeli C.M. Johnson^{d,e}, Bin Yu^c, Xin Li^{d,e}, Xuemei Chen^{a,b,f,1}**

8

9 ^aDepartment of Botany and Plant Sciences, Institute of Integrative Genome
10 Biology, University of California, Riverside, CA, 92521, USA

11 ^bGuangdong Provincial Key Laboratory for Plant Epigenetics, Longhua Institute
12 of Innovative Biotechnology, College of Life Sciences and Oceanography,
13 Shenzhen University, Shenzhen 518060, China

14 ^cSchool of Biological Sciences & Center for Plant Science Innovation, University
15 of Nebraska, Lincoln, NE, USA

16 ^dMichael Smith Laboratories, University of British Columbia, Vancouver, BC V6T
17 1Z4, Canada

18 ^eDepartment of Botany, University of British Columbia, Vancouver, BC V6T 1Z4,
19 Canada

20 ^fHoward Hughes Medical Institute, University of California, Riverside, CA 92521,
21 USA

22 ¹To whom correspondence should be addressed: Email: xuemei.chen@ucr.edu

23

24 **Short title:** MAC in RNA metabolism

25

26 **One-sentence summary:** The *Arabidopsis* MOS4-associated complex promotes
27 microRNA biogenesis and precursor messenger RNA splicing.

28

29 The author responsible for distribution of materials integral to the findings
30 presented in this article in accordance with the policy described in the
31 Instructions for Authors (www.plantcell.org) is: Dr. Xuemei Chen
32 (xuemei.chen@ucr.edu).

33

34 **ABSTRACT**

35

36 In *Arabidopsis thaliana*, the MOS4-ASSOCIATED COMPLEX (MAC) is required
37 for defense and development. The evolutionarily conserved, putative RNA
38 helicase MAC7 is a component of the *Arabidopsis* MAC and the human MAC7
39 homolog, Aquarius, is implicated in pre-mRNA splicing. Here, we show that
40 *mac7-1*, a partial loss-of-function mutant in *MAC7*, and two other MAC subunit
41 mutants, *mac3a* *mac3b* and *prl1* *prl2* (*pleiotropic regulatory locus*), exhibit
42 reduced microRNA (miRNA) levels, indicating that MAC promotes miRNA
43 biogenesis. The *mac7-1* mutant shows reduced primary miRNA (pri-miRNA)
44 levels without affecting miRNA gene (*MIR*) promoter activity or the half-life of pri-
45 miRNA transcripts. As a nuclear protein, MAC7 is not concentrated in dicing

46 bodies, but it affects the localization of HYPONASTIC LEAVES1 (HYL1), a key
47 protein in pri-miRNA processing, to dicing bodies. Immunoprecipitation of HYL1
48 retrieved eleven known MAC subunits, including MAC7, indicating association
49 between HYL1 and MAC. We propose that MAC7 links *MIR* transcription to pri-
50 miRNA processing. RNA-seq analysis showed that down-regulated genes in
51 MAC subunit mutants are mostly involved in plant defense and stimulus
52 responses, confirming a role of MAC in biotic and abiotic stress responses. We
53 also discovered global intron retention defects in mutants in three subunits of
54 MAC, thus linking MAC function to splicing in *Arabidopsis*.

55

56 INTRODUCTION

57 MicroRNAs (miRNAs) are a class of small RNAs that are approximately 20 to 24
58 nucleotides in length and act as post-transcriptional regulators of gene
59 expression in both animals and plants. MiRNAs are processed from hairpin-
60 containing precursors, primary miRNAs (pri-miRNAs), by RNase III family
61 enzymes. A mature miRNA is loaded into an Argonaute protein to form a
62 silencing complex and guides this silencing complex to target RNAs through
63 sequence complementarity with target RNAs to result in their degradation or
64 translational repression (Rogers and Chen, 2013).

65

66 The plant miRNA pathway has been intensively studied in the past decade. Early
67 studies identified key proteins with catalytic activities, including RNA polymerase
68 II (Pol II) that transcribes miRNA genes (*MIR*) (Xie et al., 2005; Zheng et al.,
69 2009), DICER-LIKE1 (DCL1), an RNase III family enzyme excising miRNAs from
70 stem-loop precursors, HUA ENHANCER1 (HEN1), a methyltransferase
71 stabilizing miRNAs by 2'-O-methylation (Park et al., 2002; Li et al., 2005; Yu et al.,
72 2005; Yang et al., 2006b; Yu et al., 2010), and ARGONAUTE 1 (AGO1), the
73 enzyme mediating miRNA-guided target RNA cleavage (Baumberger and
74 Baulcombe, 2005; Ji et al., 2011; Carbonell et al., 2012; Arribas-Hernandez et al.,
75 2016). Many factors that assist in the transcription and processing steps of
76 miRNA biogenesis have been identified (Rogers and Chen, 2013; Achkar et al.,
77 2016). Pol II-mediated *MIR* transcription requires the transcriptional coactivator
78 Mediator (Kim et al., 2011) and the transcription factor NEGATIVE ON TATA

79 LESS 2 (NOT2) (Wang et al., 2013), and is regulated by CYCLIN-DEPENDENT
80 KINASES (CDKs) (Hajheidari et al., 2012). In addition, the DNA binding protein
81 CELL DIVISION CYCLE 5 (CDC5) (Zhang et al., 2013b) and Elongator (Fang et
82 al., 2015) also regulate *MIR* transcription by Pol II.

83

84 While interacting with Pol II, NOT2, CDC5 and Elongator also interact with DCL1
85 and several DCL1-interacting proteins, and probably recruit them to pri-miRNAs
86 to facilitate their processing (Wang et al., 2013; Zhang et al., 2013b; Fang et al.,
87 2015). During the processing of miRNA precursors, DCL1 forms a dicing
88 complex with the dsRNA binding domain protein HYPONASTIC LEAVES1
89 (HYL1/DRB1), and the zinc finger protein SERRATE (SE) (Han et al., 2004;
90 Kurihara and Watanabe, 2004; Kurihara et al., 2006; Yang et al., 2006a; Dong et
91 al., 2008). DCL1 and HYL1 are enriched in subnuclear bodies, referred to as
92 dicing bodies, which are considered to be sites of miRNA precursor processing
93 (Han et al., 2004; Fang and Spector, 2007; Song et al., 2007). Many other
94 proteins also interact with DCL1 directly or indirectly in miRNA biogenesis, such
95 as Cap-Binding Proteins (CBPs) (Lambinger et al., 2008; Raczynska et al., 2014),
96 the forkhead-associated domain containing protein DAWDLE (DDL) (Yu et al.,
97 2008), the G-patch domain containing RNA binding protein TOUGH (TGH) (Ren
98 et al., 2012), and the WD-40 protein PLEIOTROPIC REGULATORY LOCUS 1
99 (PRL1) (Zhang et al., 2014). In addition, several proteins act in miRNA
100 biogenesis through the regulation of HYL1 phosphorylation, such as C-
101 TERMINAL DOMAIN PHOSPHATASE-LIKE (CPL) proteins and a K homology
102 (KH) domain protein REGULATOR OF CBF GENE EXPRESSION 3 (RCF3)
103 (Manavella et al., 2012; Karlsson et al., 2015). Several other factors, including
104 two core members of the THO/TREX complex THO2 and EMU (Furumizu et al.,
105 2010; Francisco-Mangilet et al., 2015), and the RNA binding protein MODIFIER
106 OF SNC1, 2 (MOS2) (Wu et al., 2013) do not seem to interact with any known
107 dicing complex components, but still affect miRNA biogenesis.

108

109 Among the known miRNA biogenesis factors, CDC5 and PRL1 belong to the
110 same complex, the MOS4-associated complex (MAC). MAC is a highly
111 conserved complex among eukaryotes, with its orthologs known as the
112 NINETEEN COMPLEX (NTC) or Prp19 complex (Prp19C) in yeast and humans.
113 The *Arabidopsis thaliana* MAC, yeast and human NTC/Prp19C all associate with
114 the spliceosome and are predicted to share conserved functions in splicing in all
115 three systems (Monaghan et al., 2009; Johnson et al., 2011; Koncz et al., 2012;
116 Deng et al., 2016). *Arabidopsis* CDC5 is a MYB-related transcription factor and
117 PRL1 is a conserved nuclear WD-40 protein. As core components of MAC, they
118 regulate plant development and immunity through molecular mechanisms that
119 remain unclear (Nemeth et al., 1998; Lin et al., 2007; Palma et al., 2007). They
120 both promote miRNA biogenesis but may have distinct molecular functions.
121 CDC5 binds to *MIR* promoters and interacts with DCL1 and SE to enhance
122 miRNA biogenesis (Zhang et al., 2013b), while PRL1 may stabilize pri-miRNAs
123 through its RNA binding activity and enhance DCL1 activity (Zhang et al., 2014).
124 Other *Arabidopsis* MAC subunits include two homologous proteins MAC3A and
125 MAC3B (MAC3B was shown to have E3 ligase activity *in vitro*), MAC7/Aquarius
126 (an RNA helicase), and more than ten other members (Wiborg et al., 2008;
127 Monaghan et al., 2009; Monaghan et al., 2010; Koncz et al., 2012).

128
129 *Arabidopsis* MAC7 is a putative RNA helicase, which is highly conserved in
130 eukaryotes. The human MAC7 homolog is the intron-binding protein Aquarius
131 (IBP160/AQR), which has ATPase and RNA helicase activities. It associates with
132 the spliceosome and contributes to efficient precursor-mRNA splicing *in vitro*
133 (Hirose et al., 2006; De et al., 2015). Recent publications show that EMB-4, the
134 *Caenorhabditis elegans* homolog of MAC7, physically interacts with germline
135 AGOs. It participates in the nuclear RNAi pathway and maintains the
136 homeostasis of germline transcriptome in worms (Akay et al., 2017; Tyc et al.,
137 2017). *MAC7* was predicted to be an essential gene for embryo development
138 (*EMB* gene) in *Arabidopsis* based on sequence similarity with *EMB* genes found

139 in other eukaryotes (Tzafrir et al., 2004). However, the molecular function of
140 *MAC7* remains unknown.

141
142 In this study, we performed a genetic screen using a miRNA activity reporter line,
143 the *pSUC2:amiR-SUL* (*amiR-SUL*) transgenic line (de Felippes et al., 2011). The
144 expression of *SUCROSE-PROTON SYMPORTER 2* (*SUC2*) promoter-driven
145 artificial miRNA targeting the *CHLORINA42* (*CH42*) gene creates a bleached
146 phenotype along the leaf veins. This bleaching of mesophyll cells caused by the
147 silencing effects of the artificial miRNA results in an easily scorable phenotype
148 reflecting miRNA activities in plants (de Felippes et al., 2011). From this screen,
149 we identified a point mutation in *MAC7*, *mac7-1*, as a miRNA activity suppressor
150 mutant. We showed that *MAC7* affects miRNA accumulation through promotion
151 of pri-miRNA biogenesis in *Arabidopsis*. We found that in other MAC subunit
152 mutants, including *mac3a* *mac3b* and *prl1* *prl2* double mutants, miRNA
153 biogenesis is also compromised, indicating that MAC participates in miRNA
154 biogenesis as a complex. Consistent with this, *HYL1* immunoprecipitation mass
155 spectrometry analyses revealed that *HYL1* associates with MAC *in vivo*. In
156 addition, we uncovered global intron retention defects in *mac7-1*, *mac3a* *mac3b*
157 and *prl1* *prl2* mutants through RNA-seq analysis. Our molecular characterization
158 of *MAC7* and its associated MAC components revealed their functions in miRNA
159 biogenesis and pre-mRNA splicing, which could possibly explain their roles in
160 plant development and stress responses.

161

162 **RESULTS**

163 **A silencing suppressor mutant exhibits pleiotropic phenotypes and** 164 **reduced miRNA levels**

165 To identify new players of the miRNA pathway, we performed an ethylmethane
166 sulfonate (EMS) mutagenesis screen using the *amiR-SUL* line (de Felippes et al.,
167 2011). From this screen, we identified a mutant, which we named *mac7-1* based
168 on subsequent characterization (*amiR-SUL mac7-1*) with a reduced area of
169 bleaching along the veins, indicating compromised miRNA activity (Figure 1A).

170 The mutant has pleiotropic phenotypes, such as pointed leaves, reduced root
171 length, reduced number of lateral roots, smaller plant stature and reduced fertility
172 (Figure 1B, C and Supplemental Figure 1). We crossed *amiR-SUL mac7-1* with
173 wild type (Col-0) plants to remove the *amiR-SUL* transgene. We found that the
174 *mac7-1* mutant shows the same range of phenotypes in the Col-0 background as
175 in the *amiR-SUL* background (Figure 1B, C and Supplemental Figure 1).

176

177 Because the mutant shows compromised amiR-SUL activities, we speculated
178 that reduced miRNA accumulation could be a reason. We performed RNA gel
179 blot analyses to detect amiR-SUL as well as many endogenous miRNAs. We
180 found that amiR-SUL, miR156, miR171, miR390 and many other miRNAs
181 showed reduced accumulation in both inflorescences and seedlings. The
182 reduction in miRNA abundance was small but reproducible in several biological
183 replicates (Figure 1D and Supplemental Figure 2). To assess the global influence
184 of the mutation on small RNAs, we also performed small RNA-seq with Col-0 and
185 *mac7-1* seedlings. We found that 21-nt and 24-nt small RNAs, which represent
186 the two most abundant small RNA size classes, showed a significant global
187 reduction in the *mac7-1* mutant. miRNAs showed a slight global reduction in the
188 *mac7-1* mutant but the reduction was not statistically significant (Figure 1E and
189 Supplemental Data set 1). Most miRNAs that were found to show reduced
190 abundance by RNA gel blotting also had lower levels in *mac7-1* in small RNA-
191 seq, although a few miRNAs did not (e.g. miR156, miR164) (Supplemental
192 Figure 2C). The minor inconsistency between RNA gel blotting and small RNA-
193 seq could be caused by technical limitations in small RNA-seq, e.g. bias in RNA
194 adaptor ligation or PCR amplification. Since small RNA-seq entails more
195 procedures that are prone to bias, we believe that the RNA gel blotting results
196 are more accurate.

197

198 We examined the expression of *CH42* and eight known miRNA target genes in
199 *amiR-SUL* and *amiR-SUL mac7-1*. Opposite to the reduced miRNA accumulation,

200 the expression levels of *CH42* and seven endogenous miRNA targets were
201 upregulated in *amiR-SUL mac7-1* (Figure 1F).

202

203 The reduced bleaching phenotype in *amiR-SUL mac7-1* might be attributed to
204 other factors other than, or in addition to, reduced amiR-SUL activity, e.g.
205 enhanced transcription of *CH42*. We performed RT-qPCR and immunoblotting to
206 examine *CH42* mRNA and protein levels, respectively, in Col-0 and *mac7-1* to
207 determine whether an amiR-SUL-independent effect of the *mac7-1* mutation was
208 present. While *CH42* mRNA and protein levels were both increased in *amiR-SUL*
209 *mac7-1* in comparison to *amiR-SUL*, no difference was found between Col-0 and
210 *mac7-1* (Supplemental Figure 3), indicating that the reduced bleaching
211 phenotype and elevated *CH42* expression in *amiR-SUL mac7-1* was most likely
212 caused by changes in amiR-SUL activity only.

213

214 **A point mutation in *MAC7* is responsible for the suppression of amiR-SUL-**
215 **induced silencing**

216 Through genome re-sequencing of pooled F2 mutants from a backcross between
217 *amiR-SUL mac7-1* and the parental *amiR-SUL* line, we found a C-to-T nucleotide
218 transition that changes a conserved glutamic acid to lysine (E1131K) in the open
219 reading frame (ORF) of At2g38770 (*MAC7/EMB2765*) (Figure 2A). To determine
220 whether this mutation was the causal mutation that suppressed *amiR-SUL*, we
221 first examined the linkage between the mutation and the visible phenotype. In the
222 F2 population of the backcross, we identified 84 plants with the *mac7-1*
223 phenotype, i.e., reduced vein-centered leaf bleaching. These plants were
224 genotyped for the C-to-T mutation in *MAC7*. All 84 plants were found to be
225 homozygous for this mutation, and thus the *amiR-SUL* suppressor phenotype
226 was linked with this mutation.

227

228 Next, to confirm that the causal mutation of the suppressor was in *MAC7*, we
229 generated *MAC7* promoter driven *MAC7-GFP* and *MAC7-mCherry* fusion
230 constructs, and introduced them into *mac7-1* in *amiR-SUL* and Col-0

231 backgrounds. *pMAC7:MAC7-GFP* or *pMAC7:MAC7-mCherry* fully complemented
232 the morphological defects (Figure 2B) and *pMAC7:MAC7-mCherry* restored the
233 accumulation of miRNAs of the mutant in both inflorescences and seedlings
234 (Figure 2C, D). Thus, the causal mutation in the suppressor was in *MAC7* and we
235 named this mutation *mac7-1*.

236
237 To obtain another *mac7* allele, we ordered a T-DNA insertion line, SALK_129044
238 (which we named *mac7-2*) (Supplemental Figure 4A). Genotyping *mac7-2* in the
239 progeny of a selfed *mac7-2/+* plant revealed 2:1 segregation between
240 heterozygous and wild-type plants (Supplemental Table 1), suggesting that
241 *mac7-2* homozygous plants were embryo lethal. Unlike wild-type siliques that
242 contained only normal-looking green seeds, siliques from heterozygous (*mac7-*
243 *2/+*) plants had aborted seeds that appeared pale white (Supplemental Figure
244 4B). An approximate 3:1 ratio between normal seeds and aborted seeds were
245 found (Supplemental Table 1), which was a strong indication of embryo lethality
246 of the homozygous mutant. In addition, the viability of pollen from *mac7-2/+*
247 plants appeared normal (Supplemental Figure 4C). The above evidence
248 demonstrated that *mac7-2* is a recessive, embryo-lethal mutation. As *mac7-1*
249 homozygous plants are viable, this mutation is likely a partial loss-of-function
250 allele.

251
252 The *MAC7* gene encodes an RNA helicase conserved from yeast to animals and
253 plants. The structure of the human *MAC7* ortholog, Aquarius, has been
254 determined (De et al., 2015). Based on homology modeling, we predict that the
255 plant *MAC7* also has a long N-terminal domain composed of armadillo repeats
256 (ARM), which is crucial for protein–protein interactions, a stalk and a β -barrel
257 domain, which has an architectural role, a thumb and a pointer domain, which
258 may participate in interactions with other proteins, and two RecA-like domains
259 (RecA1 and RecA2), which form a motor module required for ATP hydrolysis,
260 RNA unwinding and the coupling of these two processes. The *mac7-1* mutation
261 leads to a change of a highly conserved amino acid in the RecA1 domain, which

262 very likely affects the core functions of this protein in ATP-binding/hydrolysis and
263 nucleic acid unwinding (Figure 2A and Supplemental Figure 5) (De et al., 2015;
264 Ozgur et al., 2015).

265

266 **MAC7 promotes pri-miRNA levels without affecting *MIR* promoter activities**
267 **or pri-miRNA transcript half-life**

268 To determine the molecular mechanisms of MAC7 in miRNA biogenesis, we
269 examined the levels of pri-miRNAs. We found that the levels of pri-miRNAs from
270 many *MIR* genes were reduced in the *mac7-1* mutant (Figure 3A). This reduction
271 could be attributed to reduced transcription of *MIR* genes or enhanced pri-miRNA
272 degradation or processing. We first examined whether *mac7-1* affects *MIR*
273 promoter activities. We crossed *mac7-1* to a miRNA promoter reporter line,
274 *pMIR167a:GUS*, in which the transgene was inserted into a single genomic locus.
275 We then examined GUS activity by staining and *GUS* transcripts level by real-
276 time RT-PCR in wild-type and *mac7-1* plants, in which the transgene was
277 homozygous. There was no detectable difference between wild type and *mac7-1*
278 in terms of GUS activity or *GUS* transcripts level, indicating that *mac7-1* did not
279 affect miRNA promoter activities (Figure 3B). We also examined whether the
280 reduction of amiR-SUL level in *mac7-1* was due to reduced *SUC2* promoter
281 activity. If this was the case, we would expect the endogenous *SUC2* RNA to be
282 reduced in abundance in *mac7-1*. Real-time RT-PCR revealed that *SUC2* mRNA
283 levels did not change significantly in *mac7-1*, implying that *SUC2* promoter
284 activity was not affected by *mac7-1* and the reduction in amiR-SUL levels was
285 not due to impaired *SUC2* promoter activities in the mutant (Supplemental Figure
286 6A).

287

288 Next, we measured the half-lives of pri-miRNAs in *amiR-SUL* and *mac7-1 amiR-*
289 *SUL*. Seedlings were treated with the transcription inhibitor cordycepin, and
290 RNAs were isolated at different time points. The levels of pri-*amiR-SUL*, pri-
291 *miR167a*, and pri-*miR172a*, were determined by real-time RT-PCR. Similar half-
292 lives were found for these pri-miRNAs in the two genotypes (Figure 3C).

293
294 It is also possible that MAC7 affects miRNA biogenesis indirectly through
295 affecting the expression of key miRNA biogenesis factors. To test this possibility,
296 we determined transcript and protein levels of several key miRNA biogenesis
297 factors [i.e., DCL1, HYL1, SE, AGO1, HEN1 (transcript only)] in *amiR-SUL* and
298 *amiR-SUL mac7-1*. No differences were detected for any of the genes in the two
299 genotypes (Supplemental Figure 6B, C, D).

300
301 **MAC7 is a nuclear protein interacting with other MAC components, which**
302 **are also required for miRNA biogenesis**

303 To further characterize the molecular functions of the MAC7 protein, we
304 examined the subcellular localization of fluorescent protein tagged MAC7.
305 Transgenic plants expressing *p35S:YFP-MAC7* or *pMAC7:MAC7-GFP* exhibited
306 nuclear GFP signals (Figure 4A), which is consistent with the presence of a
307 predicted Nuclear Localization Signal (NLS) in MAC7 (Figure 2A). To determine if
308 MAC7 localized in dicing bodies, we transiently expressed YFP-MAC7 and
309 DCL1-YFP in tobacco leaves and compared their expression patterns. While
310 DCL1-YFP showed weak nucleoplasmic signals and strong dicing body signals,
311 YFP-MAC7 exhibited dispersed distribution in the nucleoplasm and was absent
312 from the nucleolus (Supplemental Figure 7A). When YFP-MAC7 was co-
313 expressed with TagRFP-HYL1, signals from the two proteins overlapped in the
314 nucleoplasm while only TagRFP-HYL1 was found concentrated in dicing bodies
315 (Supplemental Figure 7B). Immunoblot analyses confirmed the expression of
316 GFP- or YFP-tagged MAC7 in *Arabidopsis* transgenic lines (Supplemental Figure
317 7C) and in infiltrated tobacco leaves (Supplemental Figure 7D). These data
318 suggest that MAC7 does not display the dicing body patterns as DCL1 and HYL1
319 do. The dispersed nucleoplasmic distribution of MAC7 suggests broader roles
320 than miRNA biogenesis.

321
322 To uncover interacting partners of MAC7 and to determine whether MAC7
323 interacts with any known miRNA pathway proteins, we immunoprecipitated (IP)

324 MAC7 and performed mass spectrometry (MS) analyses. In one experiment, IP
325 was performed with Col-0 plants using anti-MAC7 antibodies with pre-immune
326 IgG as a negative control. In another experiment, IP was performed using
327 Chromotek-RFP-Trap with a *pMAC7:MAC7-mCherry mac7-1* line in which the
328 transgene rescued the mutant phenotypes; IP was performed using the same
329 RFP-Trap with Col-0 as a negative control. The two independent experiments
330 consistently pulled down all major MAC components, demonstrating that MAC7
331 was part of the MAC (Supplemental Table 2). An overlapping set of proteins was
332 identified from our MAC7 IP-MS and from published MOS4 IP-MS (Figure 4B and
333 Supplemental Table 2) (Monaghan et al., 2009). Besides the known MAC
334 subunits (Monaghan et al., 2009), seven additional proteins were discovered as
335 potential MAC7-associated proteins (Supplemental Table 2), but the association
336 between these proteins and MAC7, or whether they also belong to MAC, needs
337 to be further investigated.

338
339 Previous studies showed that the MAC subunits CDC5 and PRL1 promote
340 miRNA biogenesis (Zhang et al., 2013b; Zhang et al., 2014). To further confirm
341 the interactions between MAC7 with these two MAC subunits that are also
342 miRNA biogenesis factors, we performed Bimolecular Fluorescence
343 Complementation (BiFC) analysis, and found that MAC7 interacted with CDC5
344 and also interacted, albeit weakly, with PRL1 (Figure 4C). Similar BiFC studies
345 did not reveal interactions between MAC7 and HYL1 or DCL1 (Figure 4C).

346
347 These results and our work on MAC7 raise the possibility that MAC plays a role
348 in miRNA biogenesis, acting as a complex. To test this hypothesis, we examined
349 whether core subunits of MAC are required for miRNA biogenesis. Arabidopsis
350 MAC3B is a U-box E3 ubiquitin ligase, and is a core MAC component (Monaghan
351 et al., 2009). MAC3B has a homolog, MAC3A, which shares 82% identity with
352 MAC3B at the amino acid level (Monaghan et al., 2009). PRL1 is also a core
353 member of MAC. It has a homolog PRL2, which is expressed at a much lower
354 level than PRL1 (Weihmann et al., 2012). Previous studies showed that a *prl1*

355 single mutant has reduced miRNA levels but a *mac3b* mutant (SALK_050811)
356 does not (Zhang et al., 2014). Several siRNAs, ta-siRNA255 and miRNA171
357 were found to show reduced accumulation in the *mac3a mac3b* (SALK_089300
358 and SALK_050811) double mutant (Zhang et al., 2013a). Here we examined the
359 morphological and molecular phenotypes of two double mutants, *mac3a mac3b*
360 and *prl1 prl2*. Similar to other MAC subunit mutants, *mac3a mac3b* and *prl1 prl2*
361 exhibited pleiotropic developmental phenotypes (Figure 5A). RNA gel blot
362 analyses showed that miR156, miR166, and miR171 all exhibited reduced
363 accumulation in these double mutants (Figure 5B). We also performed small
364 RNA-seq with Col-0 and *prl1 prl2* seedlings to assess the global changes of
365 small RNAs in *prl1 prl2*. Similar to those of *mac7-1*, 21-nt and 24-nt small RNAs
366 showed a global reduction in *prl1 prl2*. Unlike in *mac7-1*, a significant global
367 reduction in miRNA levels was also found in *prl1 prl2*. (Figure 5C and
368 Supplemental Data Set 1). This is consistent with *mac7-1* being a weak allele
369 representing a partial compromise in MAC function. RT-qPCR analyses revealed
370 that the levels of pri-miRNAs were also reduced in *mac3a mac3b* and *prl1 prl2*
371 (Figure 5D). Thus, the molecular phenotypes of *mac3a mac3b* and *prl1 prl2*
372 mutants were similar to those of *mac7-1*.

373

374 **MAC interacts with HYL1**

375 As CDC5 and PRL1 interact with dicing complex components (Zhang et al.,
376 2013b; Zhang et al., 2014), it is possible that MAC7, or the entire MAC,
377 associates with the dicing complex. To explore the interactions between the
378 dicing complex and MAC, we performed HYL1 IP-MS. In one experiment, IP was
379 performed with a *p35S:HYL1-YFP* line and the negative control *p35S:YFP*
380 transgenic line and Col-0 using Chromotek-GFP-Trap. In another experiment, IP
381 was performed with Col-0 and the negative control *hy1-2* using anti-HYL1
382 antibodies. Eleven MAC subunits, including MAC7, were found in both IP-MS
383 experiments (Supplemental Table 3), indicating that HYL1 associates with MAC
384 *in vivo*.

385

386 The interactions between HYL1 and MAC raised the possibility that MAC7 could
387 be involved in pri-miRNA processing through affecting the dicing body
388 localization of HYL1. We crossed *mac7-1* to a *HYL1-YFP* transgenic line and
389 quantified dicing body numbers in wild type and *mac7-1*. The number of HYL1-
390 YFP-positive dicing bodies was significantly reduced in *mac7-1* compared with
391 wild type plants (Figure 6A,B), demonstrating that *MAC7* is required for the
392 proper localization of HYL1 in dicing bodies, which might partially explain the
393 compromised miRNA levels in the *mac7-1* mutant.

394

395 **Down-regulated genes in *mac* mutants are significantly related to stress
396 responses**

397 We also explored whether MAC plays a role in RNA metabolism in general. We
398 performed RNA-seq with Col-0, *mac7-1*, *mac3a mac3b*, and *prl1 prl2* seedlings
399 in two biological replicates. Differentially expressed genes (DEGs) were identified
400 between each mutant and wild type with fold change of 1.5 or more. Among the
401 three mutants, we identified 2,007 and 2,268 down-regulated (hypo-DEGs) and
402 up-regulated (hyper-DEGs) genes, respectively. 189 hypo-DEGs and 222 hyper-
403 DEGs were commonly found among *mac7-1*, *mac3a mac3b* and *prl1 prl2* (Figure
404 7 and Supplemental Data Set 2). The overlap of the DEGs among these three
405 mutants was significant (SuperExactTest, $p = 0$), indicating that these MAC
406 components function as a complex and regulate the same group of genes. The
407 large portion of non-overlapped DEGs indicates that each subunit may also have
408 its own function independent of MAC.

409

410 To understand the biological functions of MAC, we examined the Gene Ontology
411 terms enriched in the common DEGs (Gene Ontology, 2015). An enrichment of
412 genes involved in stress responses, including stimulus responses, plant defense
413 or immune responses was found in the hypo-DEGs. As for the hyper-DEGs, GO
414 terms in various small molecule biosynthetic and metabolic processes were
415 enriched (Figure 7 and Supplemental Data Set 3). Many more GO terms related
416 to stress responses were identified from the hypo-DEGs than the hyper-DEGs,

417 implying that MAC tends to activate the expression of stress response genes.
418 The results are consistent with previous findings showing that *mac3a* *mac3b* and
419 *prl1* *prl2* double mutants are more susceptible to pathogen infection (Monaghan
420 et al., 2009; Weihmann et al., 2012). To test whether *MAC7* is also required for
421 plant immunity, *mac7-1* was infected with *Pseudomonas syringae* p.v. *maculicola*
422 (*P.s.m.*) strain ES4326 together with Col-0 and *prl1-2*. The *prl1* mutants are more
423 susceptible to pathogen infection and therefore served as a positive control
424 (Weihmann et al., 2012). Pathogen growth was assayed three days after
425 bacterial inoculation. While *P.s.m.* ES4326 accumulated to higher levels in *prl1-2*
426 than in wild type, *mac7-1* was similar to wild type in terms of bacterial titer
427 (Supplemental Figure 8A). Perhaps this was due to *mac7-1* being a weak allele,
428 in which the magnitude of downregulation of the hypo-DEGs was small
429 compared to that in other *mac* mutants (Supplemental Figure 8B).

430

431 **MAC subunits affect pre-mRNA splicing**

432 Homologs of MAC in yeast and mammals play a critical role in pre-mRNA
433 splicing. In Arabidopsis, we lack evidence for a widespread role of MAC in
434 splicing; only the splicing patterns of several genes, such as *SUPPRESSOR OF*
435 *NPR1-1 CONSTITUTIVE 1* (*SNC1*) and *RESISTANCE TO PSEUDOMONAS*
436 *SYRINGAE4* (*RPS4*), were shown to be altered in several MAC subunit mutants
437 (Xu et al., 2012; Zhang et al., 2013a).

438

439 Since intron retention is a major form of alternative splicing in Arabidopsis (Ner-
440 Gaon et al., 2004), we examined whether *mac7-1*, *mac3a* *mac3b*, and *prl1* *prl2*
441 mutants had global intron retention defects. The ratio of RNA-seq reads mapping
442 to introns (including 5'/3' splice sites) and those mapping to exons only was used
443 as a measure of intron retention (see Methods for details). All annotated
444 transcripts were considered in sum as long as the read counts passed an
445 abundance filter. All three mutants exhibited significantly higher levels of intron
446 retention compared to Col-0 (Wilcoxon test, $p < 2.2e-16$) (Figure 8A and
447 Supplemental Data Set 4). Next, using the ratio of intron reads vs. exon reads as

448 a measure of intron retention levels, we identified genes with intron retention
449 defects in each mutant as compared to wild type (see Methods for details). 2819,
450 1466 and 298 genes were found to have intron retention defects in *mac3a* *mac3b*,
451 *prl1* *prl2* and *mac7-1*, respectively (Figure 8B, C and Supplemental Data Set 4).
452 Significant overlap was found among the genes with intron retention defects in
453 the three mutants (SuperExactTest, $p < 0.05$), indicating that MAC works as a
454 complex in pre-mRNA splicing (Figure 8C). Two examples of intron retention
455 events in these mutants are shown in Figure 8D.

456
457 We next examined whether there was any correlation between splicing defects
458 and gene expression. We compared the expression levels of genes with intron
459 retention defects in each mutant vs. wild type. As a reference, all genes that
460 passed a minimum intron read coverage filter (see Figure 8 legend) were
461 analyzed. There was no correlation between intron retention defects and the
462 status of their differential expression in the *mac* mutants. Like all analyzed genes,
463 genes with intron retention defects were increased, reduced, or unchanged in
464 expression levels in each mutant as compared to wild type (Figure 9A and
465 Supplemental Data Set 5). In addition, we examined intron vs. exon ratios in total
466 genes, up-regulated genes and down-regulated genes in each mutant. Both up-
467 regulated and down-regulated genes showed significant intron retention as total
468 genes (Wilcoxon test, $p < 2.2\text{e-}16$), again indicating that the intron vs. exon ratio
469 has no correlation with gene expression changes (Figure 9B and Supplemental
470 Data Set 4).

471
472 Given the intron retention defects and miRNA accumulation defects in the *mac*
473 mutants, we asked whether intron retention in pri-miRNAs contributed to the
474 miRNA accumulation defects. Many *MIR* genes were shown to have introns,
475 which are spliced out in pri-miRNAs (Laubinger et al., 2008; Zhan et al., 2012;
476 Zielezinski et al., 2015). We performed RT-PCR with intron-flanking primers to
477 detect unspliced miRNA precursors, including pri-miR163, pri-miR156, pri-
478 miR166, pri-miR168, and pri-miR172. Genomic DNA was amplified with the

479 same sets of primers to indicate the sizes of intron-containing fragments. No
480 intron retention was observed in these miRNA precursors in *mac7-1*
481 (Supplemental Figure 9).

482

483 Thus, intron retention and differential expression of genes (including *MIR* genes)
484 are not linked. MAC seems to regulate gene expression and RNA splicing
485 independently.

486

487 **DISCUSSION**

488 MAC7 is an evolutionarily conserved protein across eukaryotes, however little is
489 known about the molecular and biological functions of MAC7 or its orthologs.
490 The human ortholog Aquarius is an RNA helicase with ATPase activity, and it
491 binds to introns to assist intron splicing *in vitro* (Hirose et al., 2006; De et al.,
492 2015). The *C. elegans* ortholog EMB-4 was reported to act in the nuclear RNAi
493 pathway, where it interacts with nuclear AGOs and functions in germline-specific
494 chromatin remodeling (Checchi and Kelly, 2006; Akay et al., 2017; Tyc et al.,
495 2017). In Arabidopsis, MAC7 is involved in plant defense and was predicted to be
496 an essential gene (Tzafrir et al., 2004; Monaghan et al., 2009). In this study, we
497 showed that a T-DNA insertion mutant of *MAC7* is indeed embryo lethal, and we
498 isolated the first viable *mac7* mutant, *mac7-1*, as a miRNA biogenesis-defective
499 mutant. In this mutant, the artificial miRNA, amiR-SUL, and many endogenous
500 miRNAs show reduced accumulation. MAC7 was identified as a MAC subunit
501 through MOS4 IP-MS (Monaghan et al., 2009); our MAC7 IP-MS confirmed this.
502 Two other MAC subunits, CDC5 and PRL1, were previously shown to promote
503 miRNA biogenesis (Zhang et al., 2013b; Zhang et al., 2014). In this study, we
504 showed that MAC3 also has a similar role. Thus, it is likely that MAC as a
505 complex promotes miRNA biogenesis in general. Based on small RNA-seq
506 analysis, MAC may promote the biogenesis of not only miRNAs but also siRNAs.
507 Both 21-nt and 24-nt small RNAs, the two most abundant small RNA size classes
508 in Arabidopsis, are reduced in *mac7-1* and *prl1 prl2* mutants. A role of MAC in

509 promoting siRNA biogenesis is also supported by previous findings on CDC5,
510 MAC3 and PRL1 (Zhang et al., 2013a; Zhang et al., 2013b; Zhang et al., 2014).

511

512 How does MAC7 promote miRNA biogenesis? In *mac7-1*, the reduced
513 accumulation of miRNAs correlated with reduced levels of pri-miRNAs. Thus,
514 MAC7 probably acts in miRNA biogenesis by promoting *MIR* transcription or pri-
515 miRNA stability. However, the activity of a promoter driving *MIR* expression was
516 not affected in *mac7-1*, nor was the endogenous *SUC2* promoter activity. The
517 half-lives of pri-miRNAs were not affected either. Although we cannot exclude the
518 possibility that MAC7 promotes pri-miRNA processing into pre- or mature
519 miRNAs and prevents pri-miRNA decay at the same time and therefore pri-
520 miRNA half-lives appeared unchanged in the mutant, we prefer to hypothesize
521 that MAC7 plays a role in transcription elongation and/or maturation of pri-
522 miRNAs, considering the interactions between Pol II and MAC subunits CDC5
523 and PRL1, as well as the functions of yeast NTC in transcription elongation
524 (Kuraoka et al., 2008; Chanarat and Strasser, 2013; Zhang et al., 2013b; Zhang
525 et al., 2014). Given the role of MAC7 in pre-mRNA splicing discovered before
526 and in this study (Xu et al., 2012; Zhang et al., 2013a), we considered the
527 possibility that MAC7 acts in miRNA biogenesis by promoting the splicing of pri-
528 miRNAs. However, we did not detect intron retention in several intron-containing
529 pri-miRNAs in *mac7-1*, although the mature miRNAs from those pri-miRNAs are
530 reduced. In addition, *MIR* genes without any introns (e.g. the *pSUC2:amiR-SUL*
531 transgene, *MIR159a*, and *MIR167a*) (Szarzynska et al., 2009; de Felippes et al.,
532 2011) were also affected in *mac7-1*. Thus, the miRNA biogenesis defects of
533 *mac7-1* could not be attributed to defects in splicing. Intriguingly, we observed
534 that MAC7 affects HYL1 localization to dicing bodies. Little is known about how
535 dicing bodies form. MAC7 may recruit the dicing complex to pri-miRNAs through
536 protein–protein interactions to form dicing bodies. Alternatively, dicing complex
537 proteins are recruited by pri-miRNAs to dicing bodies, and therefore the reduced
538 number of dicing bodies in *mac7-1* could be a consequence of reduced pri-
539 miRNA levels in the mutant. We favor the second hypothesis because MAC7

540 plays a more general role in transcription and RNA metabolism (such as splicing),
541 while the dicing complex acts more specifically on miRNA precursors and is
542 presumably not recruited to other RNAs that MAC7 may also act on.

543

544 CDC5 and PRL1 were shown to interact with dicing complex proteins (e.g. DCL1,
545 SERRATE) *in vivo* through co-IP or BiFC analyses (Zhang et al., 2013b; Zhang
546 et al., 2014). We did not detect interactions between MAC7 and the dicing
547 complex through MAC7 IP-MS or BiFC analyses. However, many MAC
548 components including MAC7 were found in HYL1 IP-MS, which clearly indicates
549 association between the dicing complex and MAC *in vivo*. The possible reasons
550 for the inability of MAC7 to pull down the dicing complex proteins are: 1) The
551 interaction between MAC7 and the dicing complex is indirect or weak, and
552 bridged through CDC5 or PRL1; 2) only a small portion of MAC7 proteins
553 interacts with the dicing complex. The second hypothesis is consistent with
554 MAC7 having broader functions beyond miRNA biogenesis. We hypothesize that
555 most of HYL1 or the dicing complex is associated with MAC, but not the other
556 way around, which explains the recovery of MAC in HYL1 IP-MS.

557

558 MAC has functions beyond miRNA biogenesis in *Arabidopsis*. In our RNA-seq
559 analysis, stress response-related GO terms were significantly enriched in down-
560 regulated genes in three MAC subunit mutants. This is consistent with previous
561 studies showing that many *mac* mutants are more susceptible to pathogen
562 infection (Monaghan et al., 2009; Monaghan et al., 2010; Weihmann et al., 2012;
563 Xu et al., 2012). Although the *mac7-1* hypo-DEGs are enriched in defense
564 related GO terms, the genes show the smallest reduction magnitude compared
565 to other *mac* mutants, which could be the reason why *mac7-1* is not susceptible
566 to *P. syringae* infection as *prl1-2* and *mac3a mac3b* mutants are (Monaghan et
567 al., 2009; Weihmann et al., 2012).

568

569 It has been suspected that MAC is also involved in splicing in plants, like its
570 orthologs in human and yeast (Johnson et al., 2011; Koncz et al., 2012). Indeed,

571 our RNA-seq analyses uncovered intron retention defects in three MAC subunit
572 mutants, thus linking MAC with pre-mRNA splicing. However, there were no
573 significant correlations between intron retention and changes in gene expression.
574 Genes with intron retention were up-regulated, down-regulated, or unchanged in
575 the *mac* mutants. We also did not detect intron retention for intron-containing pri-
576 miRNAs in *mac7-1*. It is likely that MAC has separate roles in RNA splicing and
577 gene expression regulation (including the regulation of *MIR* genes). Thus, MAC
578 has broad functions in nuclear RNA metabolism.

579

580 We speculate that a common theme of MAC's role in nuclear RNA metabolism is
581 linking RNA processing to transcription (Figure 10). In yeast, the NTC promotes
582 transcription elongation (Chanarat et al., 2011; Chanarat and Strasser, 2013). In
583 both yeast and human, NTC or Prp19C associates with spliceosomes *in vivo*,
584 although this association may entail NTC subcomplexes in human (Chanarat et
585 al., 2012; De et al., 2015; Yan et al., 2015). In Arabidopsis, two MAC subunits,
586 CDC5 and PRL1, have been shown to interact with Pol II *in vivo* (Zhang et al.,
587 2013b; Zhang et al., 2014). IP-MS of an Arabidopsis spliceosome subunit also
588 pulled down multiple subunits of MAC (Deng et al., 2016). Thus, it is possible that
589 MAC promotes co-transcriptional splicing through its interactions with both Pol II
590 and the spliceosome. Similarly, in miRNA biogenesis, MAC may promote co-
591 transcriptional pri-miRNA processing through its interactions with both Pol II and
592 HYL1.

593

594 **METHODS**

595 **Plant materials and growth conditions**

596 The *pSUC2:amiR-SUL* transgenic line is a gift from Dr. Detlef Weigel (de
597 Felippes et al., 2011). *mac7-1* is a new allele isolated from our EMS mutagenesis
598 screen with the *pSUC2:amiR-SUL* transgenic line. SALK_120944 (*mac7-2*) is a
599 T-DNA insertion line obtained from the Arabidopsis Biological Resource Center
600 (ABRC). The following published transgenic lines or mutants were used:
601 *pMIR167a:GUS*, and *prl1-2* (SALK_008466) (Zhang et al., 2013b; Zhang et al.,

602 2014); *p35S:HYL1-YFP* (Qiao et al., 2015); *p35S:YFP* (Zhang et al., 2014);
603 *mac3a mac3b* (*mac3a* is SALK_089300; *mac3b* is SALK_050811) and *prl1 prl2*
604 (*prl1* is SALK_008466; *prl2* is SALK_075970) double mutants (Monaghan et al.,
605 2009; Weihmann et al., 2012).

606

607 In *pMIR167a:GUS* or *p35S:HYL1-YFP* transgenic lines, the transgene was
608 confirmed to be homozygous by Basta selection (Phosphinothricin 25mg/L, Gold
609 Biotechnology) and by examining YFP signals under fluorescence microscopy,
610 respectively, in multiple individuals. The *mac7-1* mutant was crossed into
611 *pMIR167a:GUS* or *p35S:HYL1-YFP*, and F2 plants containing homozygous
612 transgenes were confirmed in the F3 generation.

613

614 Genotyping primers used are listed in Supplemental Table 4. Plants were grown
615 in a plant growth chamber at 23°C for 16h light (Cool white fluorescent lamps,
616 25-watt Sylvania 21942 FO25/741/ECO T8 linear tube) and 8 h dark cycles.

617

618 **Mutagenesis screening and mapping of *MAC7***

619 The *amiR-SUL mac7-1* M2 mutant was backcrossed with the parental line
620 *pSUC2:amiR-SUL*. Genomic DNA was extracted from 100 pooled F2 mutants
621 and used in library construction. The library was paired-end sequenced on
622 Illumina's HiSeq 2000 at ~30x coverage, and the reads were mapped to the TAIR
623 10 genome using the Burrows-Wheeler Alignment tool (BWA) (Li and Durbin,
624 2009). SamTools (Li et al., 2009) was used to identify EMS-induced single
625 nucleotide polymorphisms (SNPs). The SNP calls generated by SamTools were
626 processed by the Next-Generation EMS mutation mapping (NGM) website tools
627 (Li et al., 2008). Two candidate mutations with 100% mutation rate were
628 identified as EMS-typical C:G to T:A transitions that are predicted to cause
629 nonsynonymous substitutions in the coding region of genes. Because one
630 candidate mutation was only supported by three reads, we focused on the one in
631 At2g38770 (*MAC7/EMB2765*), which was supported by 29 reads. A Derived
632 Cleaved Amplified Polymorphic Sequences (dCAPS) marker was designed to

633 genotype this mutation (see Supplemental Table 4 for primers). The PCR
634 products from wild type can be digested by *Eco*R1, whereas those from *mac7-1*
635 could not. Linkage analysis was performed on 84 individual mutant plants in the
636 F2 population of the backcross using this dCAPS marker to assess linkage
637 between the mutation and the *mac7-1* mutant phenotype.

638

639 **DNA constructs and complementation**

640 The *MAC7* genomic region without the stop codon was amplified and cloned into
641 pENTR/D-TOPO (Invitrogen) and then introduced to a modified pEarleyGate 301
642 vector (Earley et al., 2006) to generate *pMAC7:MAC7-mCherry* via LR reaction.
643 The *MAC7* genomic region without the stop codon was amplified and cloned into
644 the pMDC107 gateway vector (Curtis and Grossniklaus, 2003) to generate
645 *pMAC7:MAC7-GFP* with the ClonTech In-Fusion HD Cloning Kit. The *MAC7*
646 coding region was cloned and then introduced into the pEarleyGate104 vector
647 (Earley et al., 2006) via pENTR/D-TOPO (Invitrogen) through LR reactions. The
648 above plasmids were used to transform *mac7-1* plants through the
649 *Agrobacterium*-mediated floral dip method. Primers used are listed in
650 Supplemental Table 4.

651

652 **Small RNA gel blotting, RT-PCR and quantitative RT-PCR**

653 Total RNA from 2 to 3-week old seedlings (aerial part) or inflorescences was
654 extracted with TRI reagent (Molecular Research Center). RNA gel blotting for
655 detection of miRNAs was performed as described (Pall and Hamilton, 2008). 10
656 µg total RNA from aerial part of seedlings or inflorescences was used in RNA gel
657 blotting. 5' end ³²P-labelled antisense DNA oligonucleotides were used to detect
658 miRNAs. Oligonucleotide probes used are listed in Supplemental Table 4.

659

660 To perform RT-PCR, total RNA was first treated with DNase I (Roche) followed
661 by reverse transcription using RevertAid Reverse Transcriptase (Thermo Fisher
662 Scientific) with oligo-d(T) primers according to manufacturer's instructions.
663 Quantitative RT-PCR was carried out in triplicate using iQ SYBRGreen Supermix

664 (BioRad) on the BioRad CFX96 system. Primers used are listed in Supplemental
665 Table 4.

666 4

667 **RNA half-life measurements**

668 RNA half-life measurements were performed as described (Lidder et al., 2005)
669 with minor modifications. 12-day-old Col and *mac7-1* whole seedlings were
670 transferred from Murashige and Skoog medium (PhytoTechnology Lab) agar
671 plates to 6-well-plates with 1/2 MS medium and incubated overnight. The next
672 day, cordycepin (Sigma) was added to a final concentration of 0.6 mM and the
673 seedlings were collected for RNA extraction at 0, 30, 90, and 120 min after
674 cordycepin addition. RT-qPCR was then performed to determine pri-miRNA
675 levels. *UBQ5* was used as an internal control.

676

677 **Small RNA-seq library construction and data analysis**

678 To construct small RNA libraries, the aerial parts of 12-day-old Col-0, *mac7-1*,
679 and *prl1 prl2* seedlings grown on plates were harvested for total RNA extraction.
680 Two biological replicates were included: plants grown on different plates under
681 the same conditions were collected at the same time into two separate samples
682 for RNA extraction and subsequent procedures. To isolate small RNAs from total
683 RNA, 50 µg of total RNA from each sample was resolved on 15% urea-PAGE gel,
684 and the 18–30-nt region was excised from the gel. Small RNAs were recovered
685 by soaking the smashed gel in 0.3 M NaCl overnight, followed by ethanol
686 precipitation. Small RNA libraries were constructed following instructions from the
687 NEBNext Multiplex Small RNA Library Prep Set for Illumina (E7300). The
688 libraries were sequenced on an Illumina Hiseq 2500 at the UC Riverside
689 Genomics core facility.

690

691 Reads from small RNA-seq were first processed to remove the adaptor
692 sequences by cutadapt (sequence: AGATCGGAA) (Martin, 2011). The reads
693 were mapped to the TAIR10 genome using ShortStack with default parameters
694 (Johnson et al., 2016). Normalization was performed by calculating the RPMR

695 (reads per million of 45S rRNA reads) value (Li et al., 2016). Only one biological
696 replicate for Col-0 was included in this analysis since the other Col-0 sample had
697 very few reads caused by unknown problems in library construction or
698 sequencing.

699

700 **RNA-seq library construction and data analysis**

701 Polyadenylated RNA was isolated from total RNA extracted from 12-day-old
702 seedlings (aerial part) of Col-0, *mac7-1*, *mac3a mac3b*, and *prl1 prl2* using the
703 Magnetic mRNA Isolation Kit (New England Biolabs), with two biological
704 replicates for each genotype. For the biological replicates, plants grown on
705 different plates under the same conditions were collected at the same time into
706 two separate samples for RNA extraction and subsequent procedures. RNA-seq
707 libraries were prepared using NEBNext mRNA Library Prep Reagent Set for
708 Illumina (New England Biolabs) and sequenced on an Illumina Hiseq 2500
709 platform to generate high-quality single-end reads of 101bp in length. Data
710 analysis was performed with the pRNASeqTools pipeline
711 (<https://github.com/grubbybio/RNASeqTools>). Firstly, the raw reads were aligned
712 to the TAIR10 genome using HISAT2 (Kim et al., 2015). Secondly, exonic and
713 intronic reads were classified and quantified as follows. Reads with five or more
714 nucleotides overlapping with intronic regions (intronic regions defined in all
715 isoforms, including splicing donor/acceptor sites) were counted as intronic reads,
716 and reads that mapped exclusively to exonic regions were counted as exonic
717 reads. Transcript levels were measured in reads per million total read counts.
718 Differentially expressed genes were identified using DEseq2 with fold change of
719 1.5 and $p < 0.01$ as the parameters (Love et al., 2014). To identify genes that
720 exhibited significantly higher levels of intron retention compared to Col-0, the
721 intron/exon ratio was calculated as $(I_1 + I_2)/2$ over $(E_1+E_2)/2$ (I : Intronic reads, E :
722 Exonic reads, 1: biological replicate 1, 2: biological replicate 2) while applying an
723 abundance cutoff (raw intronic read number ≥ 2 and exonic read number ≥ 5).
724 We only considered intron/exon (I/E) ratios between 0 to 1. The genes with intron
725 retention were identified using DEseq2 based on values of $(I_{\text{mutant}}/E_{\text{mutant}})/(I_{\text{Col-0}}/E$

726 *Col-0*) and fold changes ≥ 2 and FDR < 0.01 as parameters (Love et al., 2014).
727 SuperExactTest was employed to access the statistical significance of DEGs or
728 intron retention gene overlaps among *mac7-1*, *mac3a* *mac3b* and *prl1* *prl2*
729 (Wang et al., 2015).

730

731 **Protein sequence alignment**

732 Database searching of MAC7 homologs was performed at National Center for
733 Biotechnology Information (NCBI) (www.ncbi.nlm.nih.gov/). Alignment of protein
734 sequence was performed with Muscle (Edgar, 2004) and the alignments were
735 edited with Jalview (Waterhouse et al., 2009).

736

737 **Antibody generation and immunoblotting**

738 To generate anti-MAC7 antibodies, a 5' portion of the coding region of *MAC7*
739 corresponding to the first 416 amino acids of the protein was amplified (primers
740 listed in Supplemental Table 4) and inserted into pMCSG7-His-MBP and
741 pSUMO-His vectors, respectively. The constructs were then transformed into the
742 *E. coli* strain BL21 for protein expression. The recombinant proteins were purified
743 by AKTA fast protein liquid chromatography (GE Healthcare) using the MBP-Trap
744 or His-Trap column. The purified MBP-tagged protein was used as antigens to
745 raise polyclonal antibodies in rabbits as described (Peterson et al., 2010). The
746 anti-serum was affinity-purified using a MAC7-SUMO-His conjugated column.
747 The purified antibodies were used in immunoblotting and IP-MS experiments.
748 Similar approach was employed to generate the anti-CH42/SUL antibody. The
749 full-length CH42 protein fused with SUMO-His tag was expressed and purified to
750 immunize two rabbits. Affinity purified antibodies were used in immunoblotting
751 analysis.

752

753 Other antibodies used in immunoblotting experiments include anti-GFP (Roche,
754 Cat. No. 11814460001), anti-AGO1 (Agrisera, AS09 527), anti-HYL1 (Agrisera,
755 AS06 136), anti-SERRATE (Agrisera, AS06 136), anti-DCL1 (Agrisera, AS12
756 2102), and anti-Tubulin (Sigma, T9026).

757

758 **Proteomic Analysis**

759 Total proteins from 12-day-old seedlings were extracted and immunoprecipitated
760 with indicated antibodies. The IP products were resolved in SDS-PAGE. The
761 antibody bands were removed and the samples were subjected to mass
762 spectrometry as described (Sleat et al., 2006; Deng et al., 2016). Two biological
763 replicated were performed, and the identified interacting proteins were those
764 represented by peptides with high hits from both biological replicates.

765

766 **Transient expression of fluorescent fusion proteins in tobacco leaf**
767 **epidermal cells**

768 The CDS of *HYL1* was amplified and cloned into pENTR/D-TOPO (Invitrogen)
769 and then introduced into the pGWB661 gateway vector (Nakamura et al., 2010)
770 to generate *p35S:TagRFP-HYL1*. *p35S:DCL1-YFP* in the pEG101 vector was
771 from a published study (Zhang et al., 2013b). The generation of *p35S:YFP-MAC7*
772 was described above. *Agrobacterium* GV3101::mp90 transformed with
773 *p35S:YFP-MAC7*, *p35S:DCL1-YFP*, or *p35S:TagRFP-HYL1* was used to infiltrate
774 tobacco leaves as described (Sparkes et al., 2006). The expression of
775 fluorescent fusion proteins was observed using a Lecia SP5 confocal laser-
776 scanning microscope.

777

778 **BiFC analysis**

779 BiFC analysis was performed as described (Walter et al., 2004). Paired cCFP
780 and nVenus constructs were co-infiltrated into *Nicotiana benthamiana* leaves.
781 After 48 h, YFP signals and chlorophyll auto fluorescence signals were excited at
782 488 nm and detected by Olympus Fluoview 500 confocal microscopy with a
783 narrow band pass filter (BA505–525 nm).

784

785 **Histochemical GUS assay and Alexander's staining of pollen**

786 GUS staining was performed as described (Kim et al., 2011). Briefly, 12-day-old
787 seedlings from Col-0 and *mac7-1* harboring a homozygous *pMIR167a:GUS*

788 transgene were vacuum infiltrated for 10 min and then incubated in GUS staining
789 solution at 37°C for several hours until blue color became visible. Tissue clearing
790 was performed with 70% ethanol for 1 to 2 days before imaging.

791
792 Alexander's staining of pollen was performed as described (Peterson et al.,
793 2010). The stained pollen grains were observed under a microscope equipped
794 with a charge-coupled device camera (Olympus).

795

796 **Accession numbers**

797 Genes referred to in this study correspond to the following Arabidopsis Genome
798 Initiative locus identifiers: *MAC7/EMB2765*, AT2G38770; *SUL/CHLORINA42*,
799 AT4G18480; *MICRORNA156A*, AT2G25095; *MICRORNA159A*, AT1G73687;
800 *MICRORNA163* AT1G66725; *MICRORNA166A* AT2G46685; *MICRORNA167A*,
801 AT3G22886; *MICRORNA168A*, AT4G19395; *MICRORNA171A*, AT3G51375;
802 *MICRORNA172A*, AT2G28056; *MICRORNA390B*, AT5G58465;
803 *MICRORNA394B*, AT1G76135; *MICRORNA396B*, AT5G35407;
804 *MICRORNA397A*, AT4G05105; *ACTIN8*, AT1G49240; *UBQUITIN5*, AT3G62250;
805 *TUBULIN3*, AT5G62700; *EIF4A1*, AT3G13920; *IPP2*, AT3G02780 ;*CDC5*,
806 AT1G09770; *PRL1*, AT4G15900; *PRL2*, AT3G16650; *MAC3A*, AT1G04510;
807 *MAC3B*, AT2G33340 ; *HYL1*, AT1G09700; *DCL1*, AT1G01040; *SERRATE*,
808 AT2G27100; *AGO1*, AT1G48410; *HEN1*, AT4G20910; *MYB33* AT5G06100;
809 *SCL6-IV* AT4G00150; *SPL10* AT1G27370; *MYB65*, AT3G11440; *ARF17*,
810 AT1G77850; *ARF8*, AT5G37020; *SCL6-III* At3g60630; *CUC2* AT5G53950.

811

812 Protein sequences of MAC7 homologs in other species correspond to the
813 following NCBI references: *Homo sapiens* intron-binding protein aquarius,
814 NP_055506.1; *Mus musculus* intron-binding protein aquarius, NP_033832.2;
815 *Danio rerio* intron-binding protein aquarius, NP_956758; *Drosophila*
816 *melanogaster* CG31368, NP_996198.2; *Caenorhabditis elegans* EMB-4,
817 NP_001256831.1; *Schizosaccharomyces pombe* *Cwf11*, NP_595360.1.

818

819 RNA sequencing data are available from NCBI Gene Expression Omnibus (GEO)
820 under the following reference numbers: Col-0_1, GSM2585832; Col-0_2,
821 GSM2585833; mac7-1_1, GSM2585834; mac7-1_2, GSM2585835;
822 mac3amac3b_1, GSM2585836; mac3amac3b_2, GSM2585837; prl1prl2_1,
823 GSM2585838; prl1prl2_2, GSM2585839; Col-0_1_sRNA GSM2771029; mac7-
824 1_1_sRNA GSM2771030; mac7-1_2_sRNA GSM2771031, prl1 prl2_1_sRNA
825 GSM2771032, prl1 prl2_2_sRNA GSM2771033.

826

827 **Supplemental Data**

828 **Supplemental Figure 1.** The *mac7-1* mutant shows pleiotropic developmental
829 phenotypes. (Supports Figure 1.)

830 **Supplemental Figure 2.** Reduced miRNA accumulation in both seedlings and
831 inflorescences in the *mac7-1* mutant. (Supports Figure 1.)

832 **Supplemental Figure 3.** The *mac7-1* mutation in the Col-0 background does not
833 affect *CH42* expression at either mRNA or protein levels. (Supports Figure 1.)

834 **Supplemental Figure 4.** The *MAC7* T-DNA insertion line, *mac7-2*, is a single-
835 locus, recessive embryo-lethal mutant. (Supports Figure 2.)

836 **Supplemental Figure 5.** Amino acid sequence alignment of *Arabidopsis* MAC7
837 orthologs. (Supports Figure 2.)

838 **Supplemental Figure 6.** MAC7 does not affect the expression of the
839 endogenous *SUC2* gene or key miRNA biogenesis factors. (Supports Figure 3.)

840 **Supplemental Figure 7.** MAC7 shows dispersed distribution in the nucleoplasm,
841 while DCL1 and HYL1 concentrate in dicing bodies in the nuclei. (Supports
842 Figure 4.)

843 **Supplemental Figure 8.** Growth of virulent *P.s.m.* ES4326 at 0 and 3 days post-
844 inoculation. (Supports Figure 7.)

845 **Supplemental Figure 9.** Intron-containing pri-miRNAs show similar splicing
846 patterns in Col-0 and *mac7-1*. (Supports Figure 8 and Figure 9.)

847 **Supplemental Table 1.** Phenotypic and genotypic segregation in the progeny of
848 selfed heterozygous *mac7-2* plants. The *mac7-2* allele harbors a T-DNA insertion
849 (SALK_129044).

850 **Supplemental Table 2.** MAC7-associated proteins identified by
851 immunoprecipitation followed by mass spectrometry.

852 **Supplemental Table 3.** HYL1-associated MAC subunits identified by
853 immunoprecipitation followed by mass spectrometry.

854 **Supplemental Table 4.** Oligonucleotide sequences.

855 **Supplemental Data Set 1.** Levels of 21-nt small RNAs, 24-nt small RNAs and
856 miRNAs in $\text{Log}_2(\text{reads per million of 45S rRNA reads})$ in Col-0, *mac7-1*, and *prl1*
857 *prl2* as determined by small RNA-seq.

858 **Supplemental Data Set 2.** Differentially expressed genes in *mac7-1*, *mac3a*
859 *mac3b*, and *prl1 prl2* mutants as determined by RNA-seq analysis.

860 **Supplemental Data Set 3.** Gene Ontology analysis of overlapped DEGs among
861 *mac7-1*, *mac3a mac3b*, and *prl1 prl2* mutants.

862 **Supplemental Data Set 4.** Intron/exon ratio in Col-0, *mac7-1*, *mac3a mac3b*,
863 and *prl1 prl2*. Genes with significantly higher intron/exon ratio as well as
864 differentially expressed genes in the mutants are shown.

865 **Supplemental Data Set 5.** Relative expression levels of genes that passed the
866 intronic and exonic read counts filter in *mac7-1*, *mac3a mac3b*, and *prl1 prl2*
867 compared to Col-0, and relative expression levels of genes with intron retention
868 defects in indicated mutants compared to Col-0.

869

870 **ACKNOWLEDGMENTS**

871 We thank Drs. Detlef Weigel and Yongli Qiao for sharing the *pSUC2:amiR-SUL* and
872 *HYL1-YFP* transgenic lines, respectively. We also thank Dr. Yongli Qiao
873 for sharing the *HYL1-YFP* transgenic line, Dr. Fedor V. Karginov for comments
874 and suggestions on this project, Dr. Brandon Le and Lorena Arroyo for technical
875 advice and support, and Dr. Haiyan Zheng for help with mass spectrometry
876 analysis. We thank Dr. Brandon Le, Dr. Shaofang Li and Yu Yu for comments on
877 this manuscript. We thank Li Liu and Dr. Wenrong He for the EMS treatment and
878 seeds planting, Dr. Jianbo Song for support for small RNA-seq analysis and
879 ZhongShou Wu for doing additional pathogen infection assays for paper revision.

880 This work was funded by the National Institutes of Health (GM061146) and
881 Gordon and Betty Moore Foundation (GBMF3046) to X.C.

882

883 **AUTHOR CONTRIBUTIONS**

884 T.J. and X.C. designed the experiments. T.J., B.Z., S.L., Y.Z., K.J., B.Y. and X.L.
885 performed the experiments. T.J., C.Y. and L.Z. analyzed the data. T.J., C.Y., and
886 X.C. wrote the manuscript.

887

887 **FIGURE LEGENDS**

888 **Figure 1. A silencing suppressor mutant *mac7-1* exhibits pleiotropic**
889 **phenotypes and compromised miRNA accumulation.**

890 (A) Differences in vein-centered bleaching in 3- to 4-week-old *pSUC2:amiR-SUL*
891 (*amiR-SUL*) and *amiR-SUL mac7-1* seedlings. (B and C) Morphological
892 phenotypes of *amiR-SUL*, *amiR-SUL mac7-1*, Col-0 and *mac7-1* plants. Images
893 of rosettes and roots were taken from 2- to 3-week-old and 1-week old plants,
894 respectively. (D) RNA gel blotting analysis of miRNAs from *amiR-SUL* and *amiR-*
895 *SUL mac7-1* inflorescences. The miRNA signals were quantified and normalized
896 to those of U6, and values were relative to *amiR-SUL* (set to 1). Two biological
897 replicates of inflorescences collected from plants grown separately but under the
898 same conditions were processed and shown. (E) Global abundance of 21-nt and
899 24-nt small RNAs and miRNAs in Col-0 and *mac7-1* as determined by small
900 RNA-seq. Small RNA libraries were generated from 12-day-old seedlings
901 growing on MS plates. The normalization of small RNAs was against 45S rRNA
902 reads and abundance was expressed as RPMR (reads per million of 45S rRNA
903 reads), and log₂ ratios of *mac7-1*/Col-0 were plotted. Asterisks indicate that the
904 mean is significantly below 0 (Wilcoxon test, p < 2.2e-16). (F) Determination of
905 miRNA target mRNA levels in *amiR-SUL* and *amiR-SUL mac7-1* using 12-day-
906 old seedlings by quantitative RT-PCR (RT-qPCR). The housekeeping gene *IPP2*
907 was included as a control. Expression levels were normalized to those of
908 *UBIQUITIN5* (*UBQ5*) and compared with those in *amiR-SUL* (set to 1). Error bars
909 indicate standard deviation from three technical replicates. Asterisks indicate
910 significant difference between Col-0 and *mac7-1* (t-test, p < 0.05).

912 **Figure 2. A point mutation in *MAC7* is responsible for the morphological**
913 **and molecular phenotypes in the *mac7-1* mutant.**

914 (A) A diagram of the MAC7 protein showing various domains, the predicted
915 nuclear localization signal (NLS), and the E1131K mutation in the *mac7-1* mutant.
916 A sequence alignment of MAC7 and its orthologs in the region containing the
917 E1131K mutation in the *mac7-1* mutant is also shown. Abbreviations for species
918 are as follows: *Arabidopsis thaliana* (A.t.), *Homo sapiens* (H.s.), *Mus musculus*
919 (M.m.), *Danio rerio* (D.r.), *Drosophila melanogaster* (D.m.), *Caenorhabditis*
920 *elegans* (C.e.), and *Schizosaccharomyces pombe* (S.p.). N: N-terminus; ARM:
921 armadillo domain; RecA: RecA-like domains; C: C-terminus. The point mutation
922 site is labeled by a triangle. (B) Morphological phenotypes of 3- to 4-week-old
923 seedlings of the indicated genotypes. *pMAC7:MAC7-GFP* and *pMAC7:MAC7-*
924 *mCherry* were transformed into *amiR-SUL mac7-1* and *mac7-1*, respectively. (C
925 and D) RNA gel blotting analysis of miRNAs from Col-0, *mac7-1*, and the
926 complementation line *mac7-1 pMAC7:MAC7-mCherry* using inflorescences (C)
927 and 12-day-old seedlings (D). The miRNA signals were quantified as described
928 in Figure 1D. RNA markers (NEB, N2102S) shown in (D) were resolved in the
929 same gel as miRNAs and probed separately by a DNA probe complementary to
930 the marker sequences.

931 **Figure 3. *MAC7* promotes pri-miRNA production.**

933 (A) Determination of pri-miRNA levels in *amiR-SUL* and *amiR-SUL mac7-1*
934 inflorescences by RT-qPCR. The housekeeping gene *IPP2* was included as a
935 control. Expression levels were normalized to those of *UBQUITIN5* (*UBQ5*) and
936 compared with those in *amiR-SUL* (set to 1). Error bars indicate standard
937 deviation from three technical replicates. Asterisks indicate significant difference
938 between *amiR-SUL* and *amiR-SUL mac7-1* (t-test, $p < 0.05$). (B) Representative
939 GUS staining images of *pMIR167a:GUS* and *mac7-1 pMIR167a:GUS* seedlings.
940 The transcript levels of *GUS* and endogenous *pri-miR167a* in *pMIR167a:GUS*
941 and *mac7-1 pMIR167a:GUS* seedlings were determined by RT-qPCR.
942 Expression levels were normalized to those of *UBQUITIN5* (*UBQ5*) and
943 compared with those in *pMIR167a:GUS* (set to 1). Error bars indicate standard
944 deviation from three technical replicates. Asterisks, t-test $p < 0.05$. (C) Half-life
945 measurements for pri-*amiR-SUL*, pri-*miR167a*, pri-*miR172a* and *EIF4A* mRNA.
946 Two-week-old *amiR-SUL* and *amiR-SUL mac7-1* seedlings were treated with 0.6
947 mM cordycepin and harvested at various time points. RT-qPCR was performed
948 to determine the levels of various pri-miRNAs and *EIF4A* mRNA. *UBQ5* served
949 as an internal control. Values at time 0 were set to 1. Error bars indicate standard
950 deviation from three technical replicates. Two biological replicates were
951 performed and similar results were obtained.
952

953 Figure 4. MAC7 is a nuclear protein associated with other MAC subunits.

954 (A) Subcellular localization of N-terminal (*p35S:YFP-MAC7*) or C-terminal
955 (*pMAC7:MAC7-GFP*) fluorescent protein tagged MAC7 in young leaves of
956 *Arabidopsis* transgenic lines. Nuclei were stained with DAPI and pseudo-colored
957 in cyan. Enlarged nuclei are shown in the insets. (B) MAC subunits identified
958 from both MAC7 and MOS4 immunoprecipitation followed by mass spectrometry
959 analysis (IP-MS). (C) BiFC analysis of MAC7 with CDC5, PRL1, HYL1 and DCL1.
960 Paired cCFP- and nVenus-fusion proteins were co-infiltrated into tobacco leaves.
961 The BiFC signal (YFP) was detected at 48 h after infiltration by confocal
962 microscopy, and was pseudo-colored in green. Magenta: auto fluorescence of
963 chlorophyll.

**964 Figure 5. The MAC subunit genes *MAC3a*, *MAC3b*, *PRL1*, and *PRL2* also
965 promote miRNA biogenesis.**

966 (A) Morphological phenotypes of 4 to 5-week old plants of the indicated
967 genotypes. (B) MiRNA levels in wild type (Col-0) and indicated mutants as
968 determined by northern blotting. The miRNA signals were quantified and
969 normalized to those of U6, and values were relative to Col-0 (arbitrarily set to 1).
970 The RNA used in northern blotting was extracted from the aerial parts of 12-day-
971 old seedlings growing on MS agar plates. (C) Global abundance of 21-nt and 24-
972 nt small RNAs and miRNAs in Col-0 and *prl1 prl2* as determined by small RNA-
973 seq. Small RNA libraries were generated from 12-day-old seedlings growing on
974 MS plates. The normalization of small RNAs was against 45S rRNA reads and
975 abundance was expressed as RPMR (reads per million of 45S rRNA reads), and
976 \log_2 ratios of *prl1 prl2*/Col-0 were plotted. Asterisks indicate that the mean is
977 significantly below 0 (Wilcoxon test, $p < 2.2e-16$). (D) Pri-miRNA levels in plants

979 of the indicated genotypes as determined by RT-qPCR. The housekeeping gene
980 *IPP2* was included as a control. *UBQ5* was used as an internal control and
981 values in Col-0 were set to 1. Error bars indicate standard deviation from three
982 technical replicates, and asterisks indicate significant difference between Col-0
983 and the mutants (t-test, $p < 0.05$).
984

985 **Figure 6. MAC7 affects HYL1 subcellular localization.**

986 (A) Images of nuclei in root cells of 7 to 10-day-old seedlings of the indicated
987 genotypes. Images (2) and (4) show five times enlarged images cropped from (1)
988 and (3), respectively. Dicing bodies are indicated by triangles. (B) The
989 percentage of cells containing HYL1-positive dicing bodies in wild type and
990 *mac7-1*. The quantification was performed by observing more than 1000 cells
991 from 27 roots for each genotype. The asterisk indicates significant difference
992 between the samples (t-test, $p < 0.05$).
993

994 **Figure 7. Down-regulated genes in the *mac* mutants are significantly
995 related to stress responses, while up-regulated genes are involved in
996 various biosynthetic and metabolic processes.**

997 (A) GO enrichment analysis of 189 commonly down-regulated genes in *mac7-1*,
998 *mac3a mac3b* and *prl1 prl2*. The degree of overlap among down-regulated genes
999 in *mac7-1*, *mac3a mac3b* and *prl1 prl2* is shown in the Venn diagram. (B) GO
1000 enrichment analysis of 222 commonly up-regulated genes *mac7-1*, *mac3a*
1001 *mac3b* and *prl1 prl2*. The degree of overlap among up-regulated genes in *mac7-1*,
1002 *mac3a mac3b* and *prl1 prl2* is shown in the Venn diagram.
1003

1004 **Figure 8. MAC subunits affect pre-mRNA splicing.**

1005 (A) Box plot of intron/exon ratios in the indicated genotypes. All genes that pass
1006 an abundance filter in expression were included in this analysis. Asterisks
1007 indicate significant difference between the mutant and wild type (Col-0)
1008 (Wilcoxon test, $p < 2.2e-16$). (B) The intron/exon ratio per gene in Col-0 vs. the
1009 indicated mutants. Black dots represent all genes with raw intronic read number
1010 ≥ 2 , exonic read number ≥ 5 , and final intron/exon ratio between 0 to 1. Red dots
1011 represent genes with significantly higher intron/exon ratio relative to wild type
1012 (fold change ≥ 2 and FDR < 0.01). (C) A Venn diagram showing the degree of
1013 overlap among genes with intron retention defects in *mac7-1*, *mac3a mac3b* and
1014 *prl1 prl2*. (D) Examples of genes with intron retention defects. RPKM: Reads Per
1015 Kilobase per Million mapped reads. Two biological replicates for each genotype
1016 are shown. The rectangles mark introns with higher retention in the mutants.
1017

1018 **Figure 9. MAC affects pre-mRNA splicing and gene expression
1019 independently.**

1020 (A) Volcano plots illustrating fold changes of gene expression levels in the
1021 indicated mutants compared to Col-0. Thresholds for fold change of 1.5 and $p \leq$
1022 0.01 are shown in the plots as gray dashed lines. Black dots and red dots
1023 represent the same genes as in Figure 8B. (B) Box plots of intron/exon ratios in
1024 total genes, up-regulated and down-regulated genes in the indicated genotypes.

1025 Only genes that pass an abundance filter (raw intronic read number ≥ 2 and
1026 exonic read number ≥ 5) were included in this analysis. Asterisks indicate
1027 significant difference between the mutant and wild type (Col-0) (Wilcoxon test, p
1028 < 2.2e-16).

1029

1030 **Figure 10. A model for MAC's functions in miRNA biogenesis and pre-
1031 mRNA processing.**

1032 MAC affects miRNA biogenesis through influencing Pol II transcription and
1033 interacting with the pri-miRNA processing factor HYL1. MAC also plays a role in
1034 pre-mRNA splicing through interactions with the spliceosome. MAC seems to
1035 have separate roles in miRNA biogenesis and RNA splicing but a common theme
1036 appears to be co-transcriptional RNA processing.

1037

1038

1039 **REFERENCES**

1040 **Achkar, N.P., Cambiagno, D.A., and Manavella, P.A.** (2016). miRNA Biogenesis: A
1041 Dynamic Pathway. *Trends Plant Sci.* **21**, 1034-1044.

1042 **Akay, A., Di Domenico, T., Suen, K.M., Nabih, A., Parada, G.E., Larance, M., Medhi, R.,**
1043 **Berkyurek, A.C., Zhang, X., Wedeles, C.J., Rudolph, K.L.M., Engelhardt, J.,**
1044 **Hemberg, M., Ma, P., Lamond, A.I., Claycomb, J.M., and Miska, E.A.** (2017). The
1045 Helicase Aquarius/EMB-4 Is Required to Overcome Intronic Barriers to Allow
1046 Nuclear RNAi Pathways to Heritably Silence Transcription. *Dev. Cell* **42**, 241-255
1047 e246.

1048 **Arribas-Hernandez, L., Marchais, A., Poulsen, C., Haase, B., Hauptmann, J., Benes, V.,**
1049 **Meister, G., and Brodersen, P.** (2016). The Slicer Activity of ARGONAUTE1 Is
1050 Required Specifically for the Phasing, Not Production, of Trans-Acting Short
1051 Interfering RNAs in Arabidopsis. *Plant Cell* **28**, 1563-1580.

1052 **Baumberger, N., and Baulcombe, D.C.** (2005). Arabidopsis ARGONAUTE1 is an RNA
1053 Slicer that selectively recruits microRNAs and short interfering RNAs. *Proc Natl*
1054 *Acad Sci U S A* **102**, 11928-11933.

1055 **Carbonell, A., Fahlgren, N., Garcia-Ruiz, H., Gilbert, K.B., Montgomery, T.A., Nguyen,**
1056 **T., Cuperus, J.T., and Carrington, J.C.** (2012). Functional analysis of three
1057 Arabidopsis ARGONAUTES using slicer-defective mutants. *Plant Cell* **24**, 3613-
1058 3629.

1059 **Chanarat, S., and Strasser, K.** (2013). Splicing and beyond: the many faces of the Prp19
1060 complex. *Biochim. Biophys. Acta* **1833**, 2126-2134.

1061 **Chanarat, S., Seizl, M., and Strasser, K.** (2011). The Prp19 complex is a novel
1062 transcription elongation factor required for TREX occupancy at transcribed
1063 genes. *Genes Dev.* **25**, 1147-1158.

1064 **Chanarat, S., Burkert-Kautzsch, C., Meinel, D.M., and Strasser, K.** (2012). Prp19C and
1065 TREX: interacting to promote transcription elongation and mRNA export.
1066 *Transcription* **3**, 8-12.

1067 **Checchi, P.M., and Kelly, W.G.** (2006). emb-4 is a conserved gene required for efficient
1068 germline-specific chromatin remodeling during *Caenorhabditis elegans*
1069 embryogenesis. *Genetics* **174**, 1895-1906.

1070 **Curtis, M.D., and Grossniklaus, U.** (2003). A gateway cloning vector set for high-
1071 throughput functional analysis of genes in planta. *Plant Physiol.* **133**, 462-469.

1072 **de Felippes, F.F., Ott, F., and Weigel, D.** (2011). Comparative analysis of non-
1073 autonomous effects of tasiRNAs and miRNAs in *Arabidopsis thaliana*. *Nucleic*
1074 *Acids Res.* **39**, 2880-2889.

1075 **De, I., Bessonov, S., Hofele, R., dos Santos, K., Will, C.L., Urlaub, H., Luhrmann, R., and**
1076 **Pena, V.** (2015). The RNA helicase Aquarius exhibits structural adaptations
1077 mediating its recruitment to spliceosomes. *Nat. Struct. Mol. Biol.* **22**, 138-144.

1078 **Deng, X., Lu, T., Wang, L., Gu, L., Sun, J., Kong, X., Liu, C., and Cao, X.** (2016).
1079 Recruitment of the NineTeen Complex to the activated spliceosome requires
1080 AtPRMT5. *Proc Natl Acad Sci U S A* **113**, 5447-5452.

1081 **Dong, Z., Han, M.H., and Fedoroff, N.** (2008). The RNA-binding proteins HYL1 and SE
1082 promote accurate in vitro processing of pri-miRNA by DCL1. *Proc Natl Acad Sci U*
1083 *S A* **105**, 9970-9975.

1084 **Earley, K.W., Haag, J.R., Pontes, O., Opper, K., Juehne, T., Song, K., and Pikaard, C.S.**
1085 (2006). Gateway-compatible vectors for plant functional genomics and
1086 proteomics. *Plant J.* **45**, 616-629.

1087 **Edgar, R.C.** (2004). MUSCLE: multiple sequence alignment with high accuracy and high
1088 throughput. *Nucleic Acids Res.* **32**, 1792-1797.

1089 **Fang, X., Cui, Y., Li, Y., and Qi, Y.** (2015). Transcription and processing of primary
1090 microRNAs are coupled by Elongator complex in Arabidopsis. *Nat Plants* **1**,
1091 15075.

1092 **Fang, Y., and Spector, D.L.** (2007). Identification of nuclear dicing bodies containing
1093 proteins for microRNA biogenesis in living Arabidopsis plants. *Curr. Biol.* **17**, 818-
1094 823.

1095 **Francisco-Mangilet, A.G., Karlsson, P., Kim, M.H., Eo, H.J., Oh, S.A., Kim, J.H.,**
1096 **Kulcheski, F.R., Park, S.K., and Manavella, P.A.** (2015). THO2, a core member of
1097 the THO/TREX complex, is required for microRNA production in Arabidopsis.
1098 *Plant J.* **82**, 1018-1029.

1099 **Furumizu, C., Tsukaya, H., and Komeda, Y.** (2010). Characterization of EMU, the
1100 Arabidopsis homolog of the yeast THO complex member HPR1. *RNA* **16**, 1809-
1101 1817.

1102 **Gene Ontology, C.** (2015). Gene Ontology Consortium: going forward. *Nucleic Acids Res.*
1103 **43**, D1049-1056.

1104 **Hajheidari, M., Farrona, S., Huettel, B., Koncz, Z., and Koncz, C.** (2012). CDKF;1 and
1105 CDKD protein kinases regulate phosphorylation of serine residues in the C-
1106 terminal domain of Arabidopsis RNA polymerase II. *Plant Cell* **24**, 1626-1642.

1107 **Han, M.H., Goud, S., Song, L., and Fedoroff, N.** (2004). The Arabidopsis double-stranded
1108 RNA-binding protein HYL1 plays a role in microRNA-mediated gene regulation.
1109 *Proc Natl Acad Sci U S A* **101**, 1093-1098.

1110 **Hirose, T., Ideue, T., Nagai, M., Hagiwara, M., Shu, M.D., and Steitz, J.A.** (2006). A
1111 spliceosomal intron binding protein, IBP160, links position-dependent assembly
1112 of intron-encoded box C/D snoRNP to pre-mRNA splicing. *Mol. Cell* **23**, 673-684.

1113 **Ji, L., Liu, X., Yan, J., Wang, W., Yumul, R.E., Kim, Y.J., Dinh, T.T., Liu, J., Cui, X., Zheng,**
1114 **B., Agarwal, M., Liu, C., Cao, X., Tang, G., and Chen, X.** (2011). ARGONAUTE10
1115 and ARGONAUTE1 regulate the termination of floral stem cells through two
1116 microRNAs in Arabidopsis. *PLoS Genet.* **7**, e1001358.

1117 **Johnson, K.C.M., Dong, O.X., and Li, X.** (2011). The evolutionarily conserved MOS4-
1118 associated complex. *Central European Journal of Biology* **6**, 776-784.

1119 **Johnson, N.R., Yeoh, J.M., Coruh, C., and Axtell, M.J.** (2016). Improved Placement of
1120 Multi-mapping Small RNAs. *G3 (Bethesda)* **6**, 2103-2111.

1121 **Karlsson, P., Christie, M.D., Seymour, D.K., Wang, H., Wang, X., Hagmann, J.,**
1122 **Kulcheski, F., and Manavella, P.A.** (2015). KH domain protein RCF3 is a tissue-
1123 biased regulator of the plant miRNA biogenesis cofactor HYL1. *Proc Natl Acad Sci*
1124 *U S A* **112**, 14096-14101.

1125 **Kim, D., Langmead, B., and Salzberg, S.L. (2015).** HISAT: a fast spliced aligner with low
1126 memory requirements. *Nat. Methods* **12**, 357-360.

1127 **Kim, Y.J., Zheng, B., Yu, Y., Won, S.Y., Mo, B., and Chen, X. (2011).** The role of Mediator
1128 in small and long noncoding RNA production in *Arabidopsis thaliana*. *EMBO J.* **30**,
1129 814-822.

1130 **Koncz, C., DeJong, F., Villacorta, N., Szakonyi, D., and Koncz, Z. (2012).** The
1131 spliceosome-activating complex: molecular mechanisms underlying the function
1132 of a pleiotropic regulator. *Front Plant Sci* **3**, 9.

1133 **Kuraoka, I., Ito, S., Wada, T., Hayashida, M., Lee, L., Saijo, M., Nakatsu, Y., Matsumoto,
1134 M., Matsunaga, T., Handa, H., Qin, J., Nakatani, Y., and Tanaka, K. (2008).**
1135 Isolation of XAB2 complex involved in pre-mRNA splicing, transcription, and
1136 transcription-coupled repair. *J. Biol. Chem.* **283**, 940-950.

1137 **Kurihara, Y., and Watanabe, Y. (2004).** *Arabidopsis* micro-RNA biogenesis through
1138 Dicer-like 1 protein functions. *Proc Natl Acad Sci U S A* **101**, 12753-12758.

1139 **Kurihara, Y., Takashi, Y., and Watanabe, Y. (2006).** The interaction between DCL1 and
1140 HYL1 is important for efficient and precise processing of pri-miRNA in plant
1141 microRNA biogenesis. *RNA* **12**, 206-212.

1142 **Laubinger, S., Sachsenberg, T., Zeller, G., Busch, W., Lohmann, J.U., Ratsch, G., and
1143 Weigel, D. (2008).** Dual roles of the nuclear cap-binding complex and SERRATE in
1144 pre-mRNA splicing and microRNA processing in *Arabidopsis thaliana*. *Proc Natl
1145 Acad Sci U S A* **105**, 8795-8800.

1146 **Li, H., and Durbin, R. (2009).** Fast and accurate short read alignment with Burrows-
1147 Wheeler transform. *Bioinformatics* **25**, 1754-1760.

1148 **Li, H., Ruan, J., and Durbin, R. (2008).** Mapping short DNA sequencing reads and calling
1149 variants using mapping quality scores. *Genome Res.* **18**, 1851-1858.

1150 **Li, H., Handsaker, B., Wysoker, A., Fennell, T., Ruan, J., Homer, N., Marth, G., Abecasis,
1151 G., Durbin, R., and Genome Project Data Processing, S. (2009).** The Sequence
1152 Alignment/Map format and SAMtools. *Bioinformatics* **25**, 2078-2079.

1153 **Li, J., Yang, Z., Yu, B., Liu, J., and Chen, X. (2005).** Methylation protects miRNAs and
1154 siRNAs from a 3'-end uridylation activity in *Arabidopsis*. *Curr. Biol.* **15**, 1501-
1155 1507.

1156 **Li, S., Le, B., Ma, X., Li, S., You, C., Yu, Y., Zhang, B., Liu, L., Gao, L., Shi, T., Zhao, Y., Mo,
1157 B., Cao, X., and Chen, X. (2016).** Biogenesis of phased siRNAs on membrane-
1158 bound polysomes in *Arabidopsis*. *Elife* **5**.

1159 **Lidder, P., Gutierrez, R.A., Salome, P.A., McClung, C.R., and Green, P.J. (2005).**
1160 Circadian control of messenger RNA stability. Association with a sequence-
1161 specific messenger RNA decay pathway. *Plant Physiol.* **138**, 2374-2385.

1162 **Lin, Z., Yin, K., Zhu, D., Chen, Z., Gu, H., and Qu, L.J. (2007).** AtCDC5 regulates the G2 to
1163 M transition of the cell cycle and is critical for the function of *Arabidopsis* shoot
1164 apical meristem. *Cell Res.* **17**, 815-828.

1165 **Love, M.I., Huber, W., and Anders, S. (2014).** Moderated estimation of fold change and
1166 dispersion for RNA-seq data with DESeq2. *Genome Biol* **15**, 550.

1167 **Manavella, P.A., Hagmann, J., Ott, F., Laubinger, S., Franz, M., Macek, B., and Weigel, D.** (2012). Fast-forward genetics identifies plant CPL phosphatases as regulators
1168 of miRNA processing factor HYL1. *Cell* **151**, 859-870.

1169

1170 **Martin, M.** (2011). Cutadapt removes adapter sequences from high-throughput
1171 sequencing reads. *EMBnet.journal* **17**, 10-12.

1172 **Monaghan, J., Xu, F., Xu, S., Zhang, Y., and Li, X.** (2010). Two putative RNA-binding
1173 proteins function with unequal genetic redundancy in the MOS4-associated
1174 complex. *Plant Physiol.* **154**, 1783-1793.

1175 **Monaghan, J., Xu, F., Gao, M., Zhao, Q., Palma, K., Long, C., Chen, S., Zhang, Y., and Li, X.** (2009). Two Prp19-like U-box proteins in the MOS4-associated complex play
1176 redundant roles in plant innate immunity. *PLoS Pathog* **5**, e1000526.

1177

1178 **Nakamura, S., Mano, S., Tanaka, Y., Ohnishi, M., Nakamori, C., Araki, M., Niwa, T., Nishimura, M., Kaminaka, H., Nakagawa, T., Sato, Y., and Ishiguro, S.** (2010). Gateway binary vectors with the bialaphos resistance gene, bar, as a selection
1179 marker for plant transformation. *Biosci Biotechnol Biochem* **74**, 1315-1319.

1180

1181 **Nemeth, K., Salchert, K., Putnoky, P., Bhalerao, R., Koncz-Kalman, Z., Stankovic-Stangeland, B., Bako, L., Mathur, J., Okresz, L., Stabel, S., Geigenberger, P., Stitt, M., Redei, G.P., Schell, J., and Koncz, C.** (1998). Pleiotropic control of
1182 glucose and hormone responses by PRL1, a nuclear WD protein, in *Arabidopsis*. *Genes Dev.* **12**, 3059-3073.

1183

1184 **Ner-Gaon, H., Halachmi, R., Savaldi-Goldstein, S., Rubin, E., Ophir, R., and Fluhr, R.** (2004). Intron retention is a major phenomenon in alternative splicing in
1185 *Arabidopsis*. *Plant J.* **39**, 877-885.

1186

1187 **Ozgur, S., Buchwald, G., Falk, S., Chakrabarti, S., Prabu, J.R., and Conti, E.** (2015). The
1188 conformational plasticity of eukaryotic RNA-dependent ATPases. *FEBS J.* **282**,
1189 850-863.

1190

1191 **Pall, G.S., and Hamilton, A.J.** (2008). Improved northern blot method for enhanced
1192 detection of small RNA. *Nat Protoc* **3**, 1077-1084.

1193

1194 **Palma, K., Zhao, Q., Cheng, Y.T., Bi, D., Monaghan, J., Cheng, W., Zhang, Y., and Li, X.** (2007). Regulation of plant innate immunity by three proteins in a complex
1195 conserved across the plant and animal kingdoms. *Genes Dev.* **21**, 1484-1493.

1196

1197 **Park, W., Li, J., Song, R., Messing, J., and Chen, X.** (2002). CARPEL FACTORY, a Dicer
1198 homolog, and HEN1, a novel protein, act in microRNA metabolism in *Arabidopsis*
1199 thaliana. *Curr. Biol.* **12**, 1484-1495.

1200

1201 **Peterson, R., Slovin, J.P., and Chen, C.** (2010). A simplified method for differential
1202 staining of aborted and non-aborted pollen grains. *Int J Plant Biol* **1:e13**, 66-69.

1203

1204 **Qiao, Y., Shi, J., Zhai, Y., Hou, Y., and Ma, W.** (2015). Phytophthora effector targets a
1205 novel component of small RNA pathway in plants to promote infection. *Proc Natl
Acad Sci U S A* **112**, 5850-5855.

1206

1207 **Raczynska, K.D., Stepien, A., Kierzkowski, D., Kalak, M., Bajczyk, M., McNicol, J., Simpson, C.G., Szwedkowska-Kulinska, Z., Brown, J.W., and Jarmolowski, A.** (2014). The SERRATE protein is involved in alternative splicing in *Arabidopsis*
1208 thaliana. *Nucleic Acids Res.* **42**, 1224-1244.

1209

1210 **Ren, G., Xie, M., Dou, Y., Zhang, S., Zhang, C., and Yu, B.** (2012). Regulation of miRNA
1211 abundance by RNA binding protein TOUGH in Arabidopsis. *Proc Natl Acad Sci U S*
1212 **A** **109**, 12817-12821.

1213 **Rogers, K., and Chen, X.** (2013). Biogenesis, turnover, and mode of action of plant
1214 microRNAs. *Plant Cell* **25**, 2383-2399.

1215 **Sleat, D.E., Zheng, H., Qian, M., and Lobel, P.** (2006). Identification of sites of mannose
1216 6-phosphorylation on lysosomal proteins. *Mol. Cell. Proteomics* **5**, 686-701.

1217 **Song, L., Han, M.H., Lesicka, J., and Fedoroff, N.** (2007). Arabidopsis primary microRNA
1218 processing proteins HYL1 and DCL1 define a nuclear body distinct from the Cajal
1219 body. *Proc Natl Acad Sci U S A* **104**, 5437-5442.

1220 **Sparkes, I.A., Runions, J., Kearns, A., and Hawes, C.** (2006). Rapid, transient expression
1221 of fluorescent fusion proteins in tobacco plants and generation of stably
1222 transformed plants. *Nat Protoc* **1**, 2019-2025.

1223 **Szarzynska, B., Sobkowiak, L., Pant, B.D., Balazadeh, S., Scheible, W.R., Mueller-
1224 Roeber, B., Jarmolowski, A., and Szwedkowska-Kulinska, Z.** (2009). Gene
1225 structures and processing of Arabidopsis thaliana HYL1-dependent pri-miRNAs.
1226 *Nucleic Acids Res.* **37**, 3083-3093.

1227 **Tyc, K.M., Nabih, A., Wu, M.Z., Wedeles, C.J., Sobotka, J.A., and Claycomb, J.M.** (2017).
1228 The Conserved Intron Binding Protein EMB-4 Plays Differential Roles in Germline
1229 Small RNA Pathways of *C. elegans*. *Dev. Cell* **42**, 256-270 e256.

1230 **Tzafrir, I., Pena-Muralla, R., Dickerman, A., Berg, M., Rogers, R., Hutchens, S.,
1231 Sweeney, T.C., McElver, J., Aux, G., Patton, D., and Meinke, D.** (2004).
1232 Identification of genes required for embryo development in Arabidopsis. *Plant
1233 Physiol.* **135**, 1206-1220.

1234 **Walter, M., Chaban, C., Schutze, K., Batistic, O., Weckermann, K., Nake, C., Blazevic,
1235 D., Grefen, C., Schumacher, K., Oecking, C., Harter, K., and Kudla, J.** (2004).
1236 Visualization of protein interactions in living plant cells using bimolecular
1237 fluorescence complementation. *Plant J.* **40**, 428-438.

1238 **Wang, L., Song, X., Gu, L., Li, X., Cao, S., Chu, C., Cui, X., Chen, X., and Cao, X.** (2013).
1239 NOT2 proteins promote polymerase II-dependent transcription and interact with
1240 multiple MicroRNA biogenesis factors in Arabidopsis. *Plant Cell* **25**, 715-727.

1241 **Wang, M., Zhao, Y., and Zhang, B.** (2015). Efficient Test and Visualization of Multi-Set
1242 Intersections. *Sci Rep* **5**, 16923.

1243 **Waterhouse, A.M., Procter, J.B., Martin, D.M., Clamp, M., and Barton, G.J.** (2009).
1244 Jalview Version 2--a multiple sequence alignment editor and analysis workbench.
1245 *Bioinformatics* **25**, 1189-1191.

1246 **Weihmann, T., Palma, K., Nitta, Y., and Li, X.** (2012). Pleiotropic regulatory locus 2
1247 exhibits unequal genetic redundancy with its homolog PRL1. *Plant Cell Physiol.*
1248 **53**, 1617-1626.

1249 **Wiborg, J., O'Shea, C., and Skriver, K.** (2008). Biochemical function of typical and variant
1250 Arabidopsis thaliana U-box E3 ubiquitin-protein ligases. *Biochem. J.* **413**, 447-
1251 457.

1252 **Wu, X., Shi, Y., Li, J., Xu, L., Fang, Y., Li, X., and Qi, Y.** (2013). A role for the RNA-binding
1253 protein MOS2 in microRNA maturation in Arabidopsis. *Cell Res.* **23**, 645-657.

1254 **Xie, Z., Allen, E., Fahlgren, N., Calamar, A., Givan, S.A., and Carrington, J.C. (2005).**
1255 Expression of *Arabidopsis* MIRNA genes. *Plant Physiol.* **138**, 2145-2154.

1256 **Xu, F., Xu, S., Wiermer, M., Zhang, Y., and Li, X. (2012).** The cyclin L homolog MOS12
1257 and the MOS4-associated complex are required for the proper splicing of plant
1258 resistance genes. *Plant J.* **70**, 916-928.

1259 **Yan, C., Hang, J., Wan, R., Huang, M., Wong, C.C., and Shi, Y. (2015).** Structure of a
1260 yeast spliceosome at 3.6-angstrom resolution. *Science* **349**, 1182-1191.

1261 **Yang, L., Liu, Z., Lu, F., Dong, A., and Huang, H. (2006a).** SERRATE is a novel nuclear
1262 regulator in primary microRNA processing in *Arabidopsis*. *Plant J.* **47**, 841-850.

1263 **Yang, Z., Ebright, Y.W., Yu, B., and Chen, X. (2006b).** HEN1 recognizes 21-24 nt small
1264 RNA duplexes and deposits a methyl group onto the 2' OH of the 3' terminal
1265 nucleotide. *Nucleic Acids Res.* **34**, 667-675.

1266 **Yu, B., Yang, Z., Li, J., Minakhina, S., Yang, M., Padgett, R.W., Steward, R., and Chen, X.**
1267 (2005). Methylation as a crucial step in plant microRNA biogenesis. *Science* **307**,
1268 932-935.

1269 **Yu, B., Bi, L., Zhai, J., Agarwal, M., Li, S., Wu, Q., Ding, S.W., Meyers, B.C., Vaucheret,**
1270 **H., and Chen, X. (2010).** siRNAs compete with miRNAs for methylation by HEN1
1271 in *Arabidopsis*. *Nucleic Acids Res.* **38**, 5844-5850.

1272 **Yu, B., Bi, L., Zheng, B., Ji, L., Chevalier, D., Agarwal, M., Ramachandran, V., Li, W.,**
1273 **Lagrange, T., Walker, J.C., and Chen, X. (2008).** The FHA domain proteins
1274 DAWDLE in *Arabidopsis* and SNIP1 in humans act in small RNA biogenesis. *Proc*
1275 *Natl Acad Sci U S A* **105**, 10073-10078.

1276 **Zhan, X., Wang, B., Li, H., Liu, R., Kalia, R.K., Zhu, J.K., and Chinnusamy, V. (2012).**
1277 *Arabidopsis* proline-rich protein important for development and abiotic stress
1278 tolerance is involved in microRNA biogenesis. *Proc Natl Acad Sci U S A* **109**,
1279 18198-18203.

1280 **Zhang, C.J., Zhou, J.X., Liu, J., Ma, Z.Y., Zhang, S.W., Dou, K., Huang, H.W., Cai, T., Liu,**
1281 **R., Zhu, J.K., and He, X.J. (2013a).** The splicing machinery promotes RNA-
1282 directed DNA methylation and transcriptional silencing in *Arabidopsis*. *EMBO J.*
1283 **32**, 1128-1140.

1284 **Zhang, S., Liu, Y., and Yu, B. (2014).** PRL1, an RNA-binding protein, positively regulates
1285 the accumulation of miRNAs and siRNAs in *Arabidopsis*. *PLoS Genet.* **10**,
1286 e1004841.

1287 **Zhang, S., Xie, M., Ren, G., and Yu, B. (2013b).** CDC5, a DNA binding protein, positively
1288 regulates posttranscriptional processing and/or transcription of primary
1289 microRNA transcripts. *Proc Natl Acad Sci U S A* **110**, 17588-17593.

1290 **Zheng, B., Wang, Z., Li, S., Yu, B., Liu, J.Y., and Chen, X. (2009).** Intergenic transcription
1291 by RNA polymerase II coordinates Pol IV and Pol V in siRNA-directed
1292 transcriptional gene silencing in *Arabidopsis*. *Genes Dev.* **23**, 2850-2860.

1293 **Zielezinski, A., Dolata, J., Alaba, S., Kruszka, K., Pacak, A., Swida-Barteczka, A., Knop,**
1294 **K., Stepień, A., Bielewicz, D., Pietrykowska, H., Sierocka, I., Sobkowiak, L.,**
1295 **Lakomiak, A., Jarmolowski, A., Szwedkowska-Kulinska, Z., and Karłowski, W.M.**
1296 (2015). mirEX 2.0 - an integrated environment for expression profiling of plant
1297 microRNAs. *BMC Plant Biol.* **15**, 144.

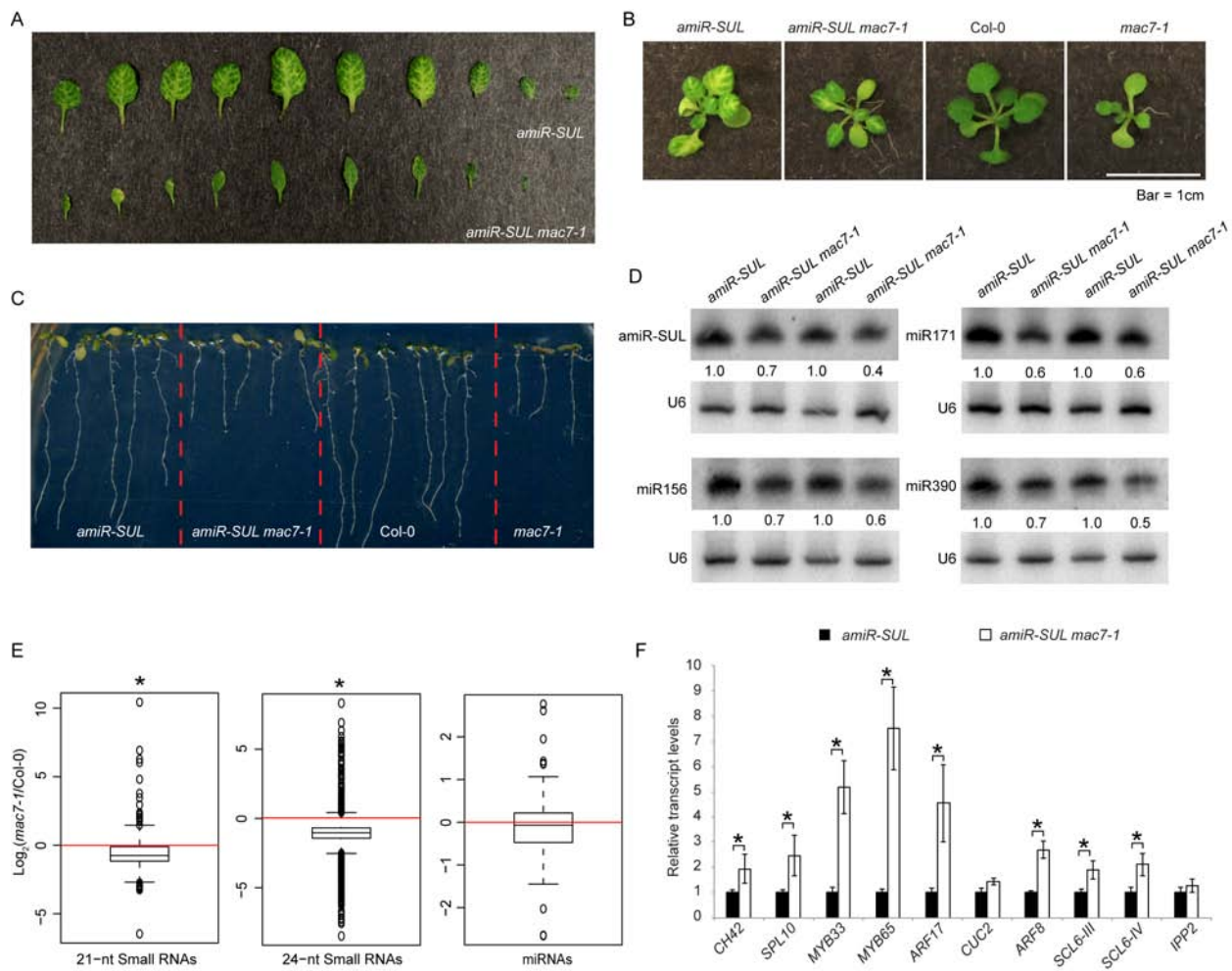


Figure 1. A silencing suppressor mutant *mac7-1* exhibits pleiotropic phenotypes and compromised miRNA accumulation.

(A) Differences in vein-centered bleaching in 3 to 4-week old *pSUC2:amiR-SUL* (*amiR-SUL*) and *amiR-SUL mac7-1* seedlings. (B and C) Morphological phenotypes of *amiR-SUL*, *amiR-SUL mac7-1*, *Col-0* and *mac7-1* plants. Images of rosettes and roots were taken from 2 to 3-week old and 1-week old plants, respectively. (D) Northern blotting analysis of miRNAs from *amiR-SUL* and *amiR-SUL mac7-1* inflorescences. The miRNA signals were quantified and normalized to those of U6, and values were relative to *amiR-SUL* (arbitrarily set to 1). Two biological replicates of inflorescences collected from plants grown separately but under the same conditions were processed and shown. (E) Global abundance of 21-nt and 24-nt small RNAs and miRNAs in *Col-0* and *mac7-1* as determined by small RNA-seq. Small RNA libraries were generated from 12-day-old seedlings growing on MS plates. The normalization of small RNAs was against 45S rRNA reads and abundance was expressed as RPMR (reads per million of 45S rRNA reads), and log₂ ratios of *mac7-1*/Col-0 were plotted. Asterisks indicate that the mean is significantly below 0 (Wilcoxon test, $p < 2.2e-16$). (F) Determination of miRNA target mRNA levels in *amiR-SUL* and *amiR-SUL mac7-1* using 12-day-old seedlings by quantitative RT-PCR (RT-qPCR). The housekeeping gene *IPP2* was included as a control. Expression levels were normalized to those of *UBQUITIN5* (*UBQ5*) and compared with those in *amiR-SUL* (set to 1). Error bars indicate standard deviation from three technical replicates. Asterisks indicate significant difference between *Col-0* and *mac7-1* (t-test, $p < 0.05$).

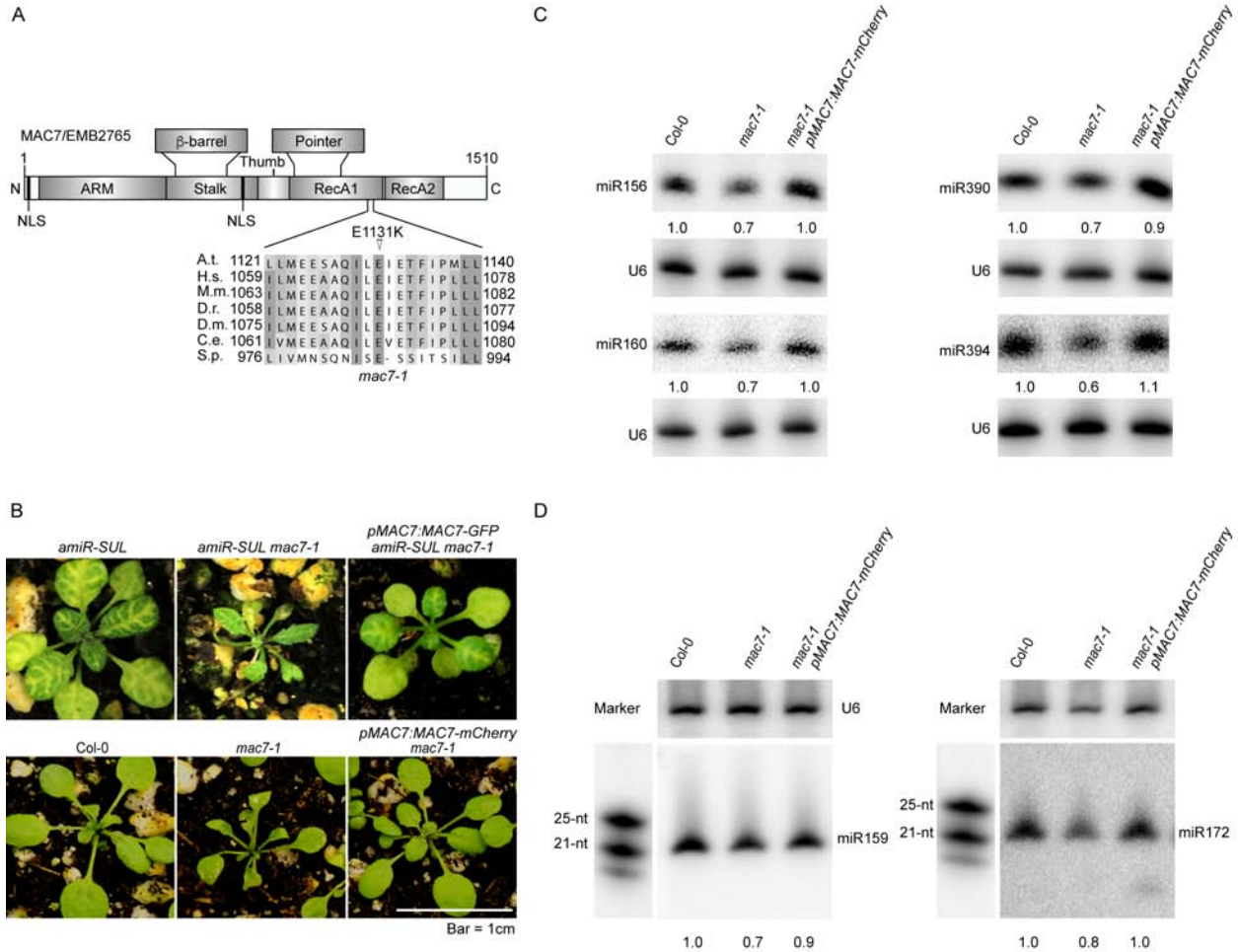


Figure 2. A point mutation in *MAC7* is responsible for the morphological and molecular phenotypes in the *mac7-1* mutant.

(A) A diagram of the MAC7 protein showing various domains, the predicted nuclear localization signal (NLS), and the E1131K mutation in the *mac7-1* mutant. A sequence alignment of MAC7 and its orthologs in the region containing the E1131K mutation in the *mac7-1* mutant is also shown. Abbreviations for species are as follows: *Arabidopsis thaliana* (A.t.), *Homo sapiens* (H.s.), *Mus musculus* (M.m.), *Danio rerio* (D.r.), *Drosophila melanogaster* (D.m.), *Caenorhabditis elegans* (C.e.), and *Schizosaccharomyces pombe* (S.p.). N: N-terminus; ARM: armadillo domain; RecA: RecA-like domains; C: C-terminus. The point mutation site is labeled by a triangle. (B) Morphological phenotypes of 3 to 4-week old seedlings of the indicated genotypes. *pMAC7:MAC7-GFP* and *pMAC7:MAC7-mCherry* were transformed into *amiR-SUL mac7-1* and *mac7-1*, respectively. (C and D) Northern blotting analysis of miRNAs from Col-0, *mac7-1*, and the complementation line *mac7-1 pMAC7:MAC7-mCherry* using inflorescences (C) and 12-day-old seedlings (D). The miRNA signals were quantified as described in Figure 1D. RNA markers (NEB, N2102S) shown in (D) were resolved in the same gel as miRNAs and probed separately by a DNA probe complementary to the marker sequences.

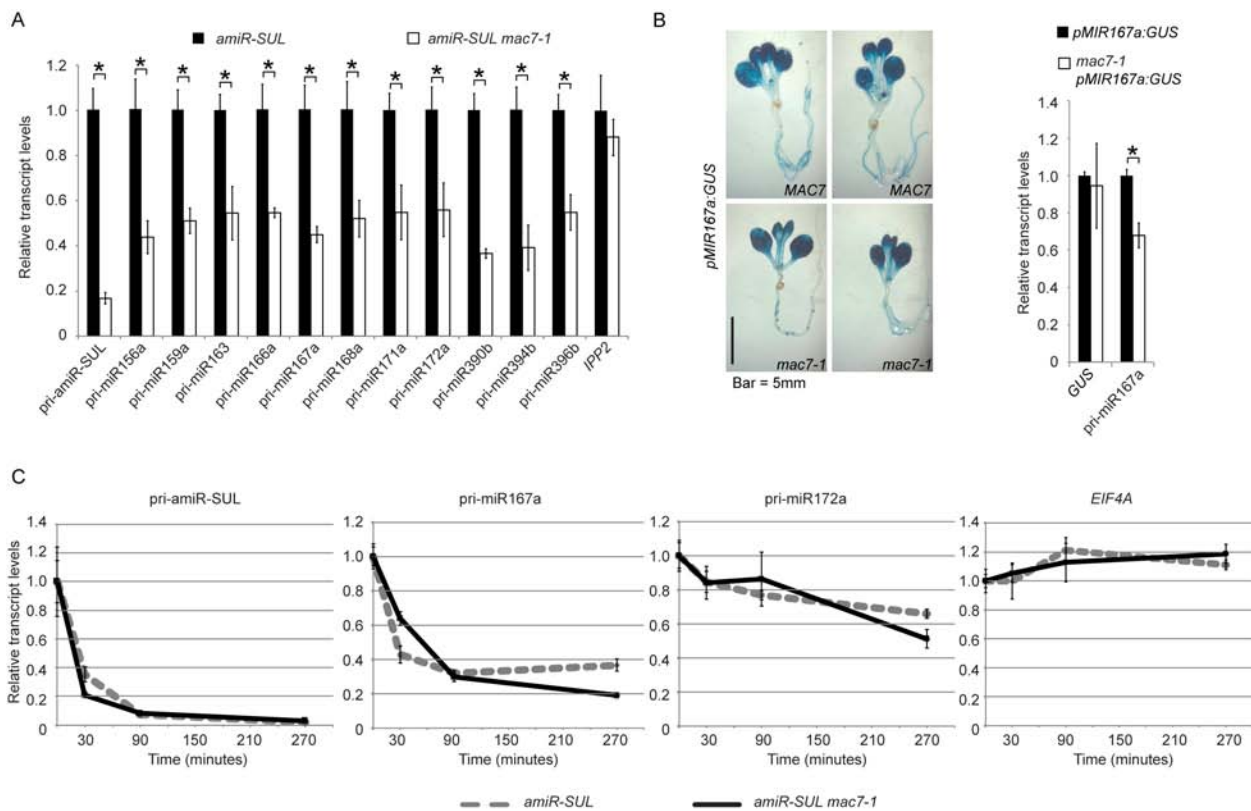


Figure 3. MAC7 promotes pri-miRNA production.

(A) Determination of pri-miRNA levels in *amiR-SUL* and *amiR-SUL mac7-1* inflorescences by RT-qPCR. The housekeeping gene *IPP2* was included as a control. Expression levels were normalized to those of *UBQUITIN5* (*UBQ5*) and compared with those in *amiR-SUL* (set to 1). Error bars indicate standard deviation from three technical replicates. Asterisks indicate significant difference between *amiR-SUL* and *amiR-SUL mac7-1* (t-test, $p < 0.05$). (B) Representative GUS staining images of *pMIR167a:GUS* and *mac7-1 pMIR167a:GUS* seedlings. The transcript levels of *GUS* and endogenous *pri-miR167a* in *pMIR167a:GUS* and *mac7-1 pMIR167a:GUS* seedlings were determined by RT-qPCR. Expression levels were normalized to those of *UBQUITIN5* (*UBQ5*) and compared with those in *pMIR167a:GUS* (set to 1). Error bars indicate standard deviation from three technical replicates. Asterisks, t-test $p < 0.05$. (C) Half-life measurements for pri-amiR-SUL, pri-miR167a, pri-miR172a and *EIF4A* mRNA. Two-week-old *amiR-SUL* and *amiR-SUL mac7-1* seedlings were treated with 0.6 mM cordycepin and harvested at various time points. RT-qPCR was performed to determine the levels of various pri-miRNAs and *EIF4A* mRNA. *UBQ5* served as an internal control. Values at time 0 were set to 1. Error bars indicate standard deviation from three technical replicates. Two biological replicates were performed and similar results were obtained.

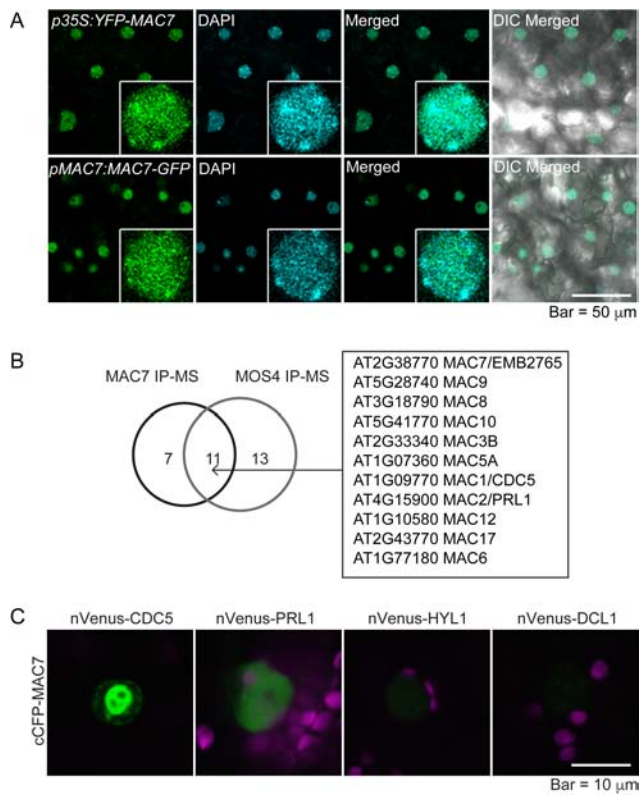


Figure 4. MAC7 is a nuclear protein associated with other MAC subunits.

(A) Subcellular localization of N-terminal (*p35S:YFP-MAC7*) or C-terminal (*pMAC7:MAC7-GFP*) fluorescent protein tagged MAC7 in young leaves of *Arabidopsis* transgenic lines. Nuclei were stained with DAPI and pseudo-colored in cyan. Enlarged nuclei are shown in the insets. (B) MAC subunits identified from both MAC7 and MOS4 immunoprecipitation followed by mass spectrometry analysis (IP-MS). (C) BiFC analysis of MAC7 with CDC5, PRL1, HYL1 and DCL1. Paired cCFP- and nVenus-fusion proteins were co-infiltrated into tobacco leaves. The BiFC signal (YFP) was detected at 48 h after infiltration by confocal microscopy, and was pseudo-colored in green. Magenta: auto fluorescence of chlorophyll.

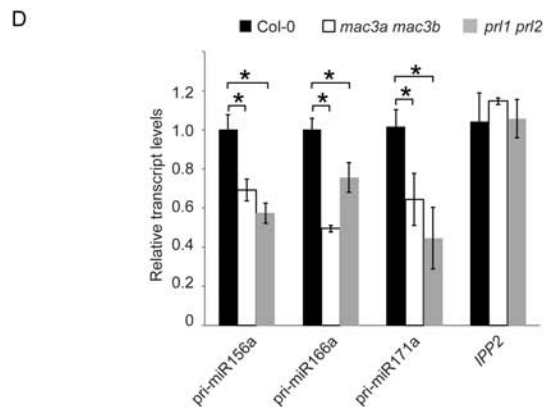
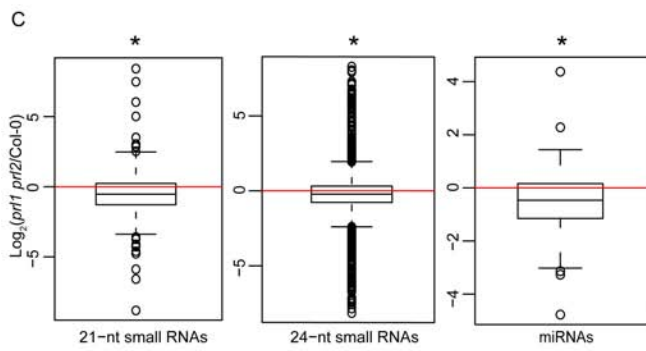
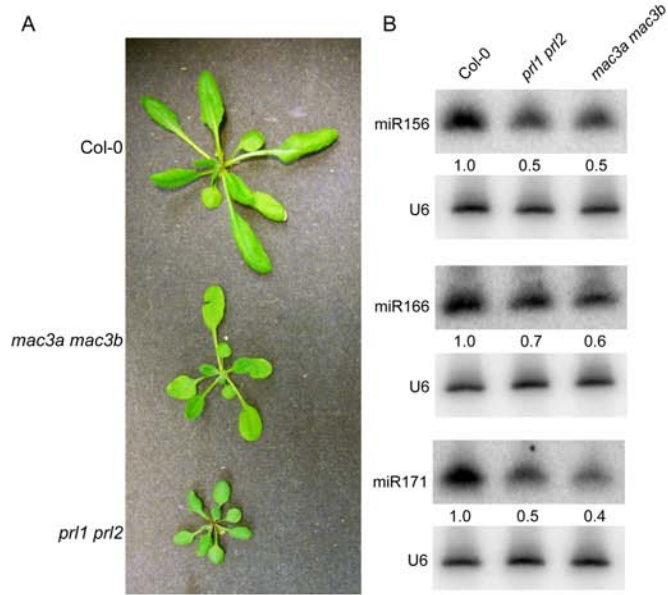


Figure 5. The MAC subunit genes *MAC3a*, *MAC3b*, *PRL1*, and *PRL2* also promote miRNA biogenesis.

(A) Morphological phenotypes of 4 to 5-week old plants of the indicated genotypes. (B) MiRNA levels in wild type (Col-0) and indicated mutants as determined by northern blotting. The miRNA signals were quantified and normalized to those of U6, and values were relative to Col-0 (arbitrarily set to 1). The RNA used in northern blotting was extracted from the aerial parts of 12-day-old seedlings growing on MS agar plates. (C) Global abundance of 21-nt and 24-nt small RNAs and miRNAs in Col-0 and *prl1 prl2* as determined by small RNA-seq. Small RNA libraries were generated from 12-day-old seedlings growing on MS plates. The normalization of small RNAs was against 45S rRNA reads and abundance was expressed as RPMR (reads per million of 45S rRNA reads), and \log_2 ratios of *prl1 prl2*/Col-0 were plotted. Asterisks indicate that the mean is significantly below 0 (Wilcoxon test, $p < 2.2\text{e-}16$). (D) Pri-miRNA levels in plants of the indicated genotypes as determined by RT-qPCR. The housekeeping gene *IPP2* was included as a control. *UBQ5* was used as an internal control and values in Col-0 were set to 1. Error bars indicate standard deviation from three technical replicates, and asterisks indicate significant difference between Col-0 and the mutants (t-test, $p < 0.05$).

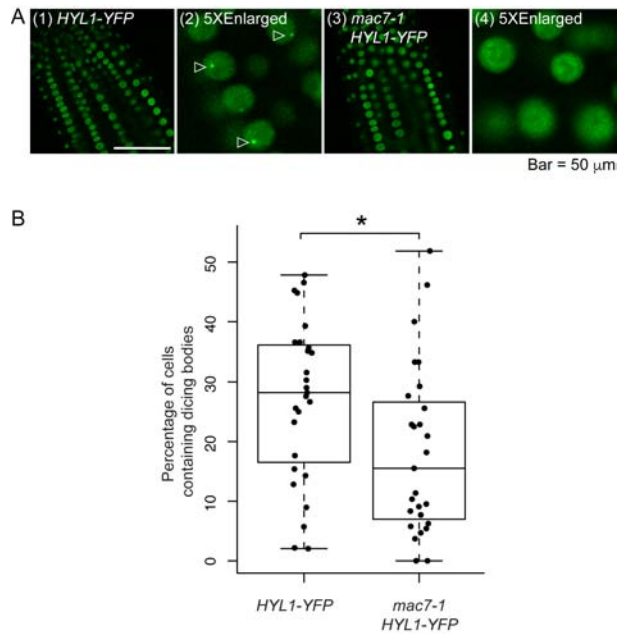


Figure 6. MAC7 affects HYL1 subcellular localization.

(A) Images of nuclei in root cells of 7 to 10-day-old seedlings of the indicated genotypes. Images (2) and (4) show five times enlarged images cropped from (1) and (3), respectively. Dicing bodies are indicated by triangles. (B) The percentage of cells containing HYL1-positive dicing bodies in wild type and *mac7-1*. The quantification was performed by observing more than 1000 cells from 27 roots for each genotype. The asterisk indicates significant difference between the samples (t-test, $p < 0.05$).

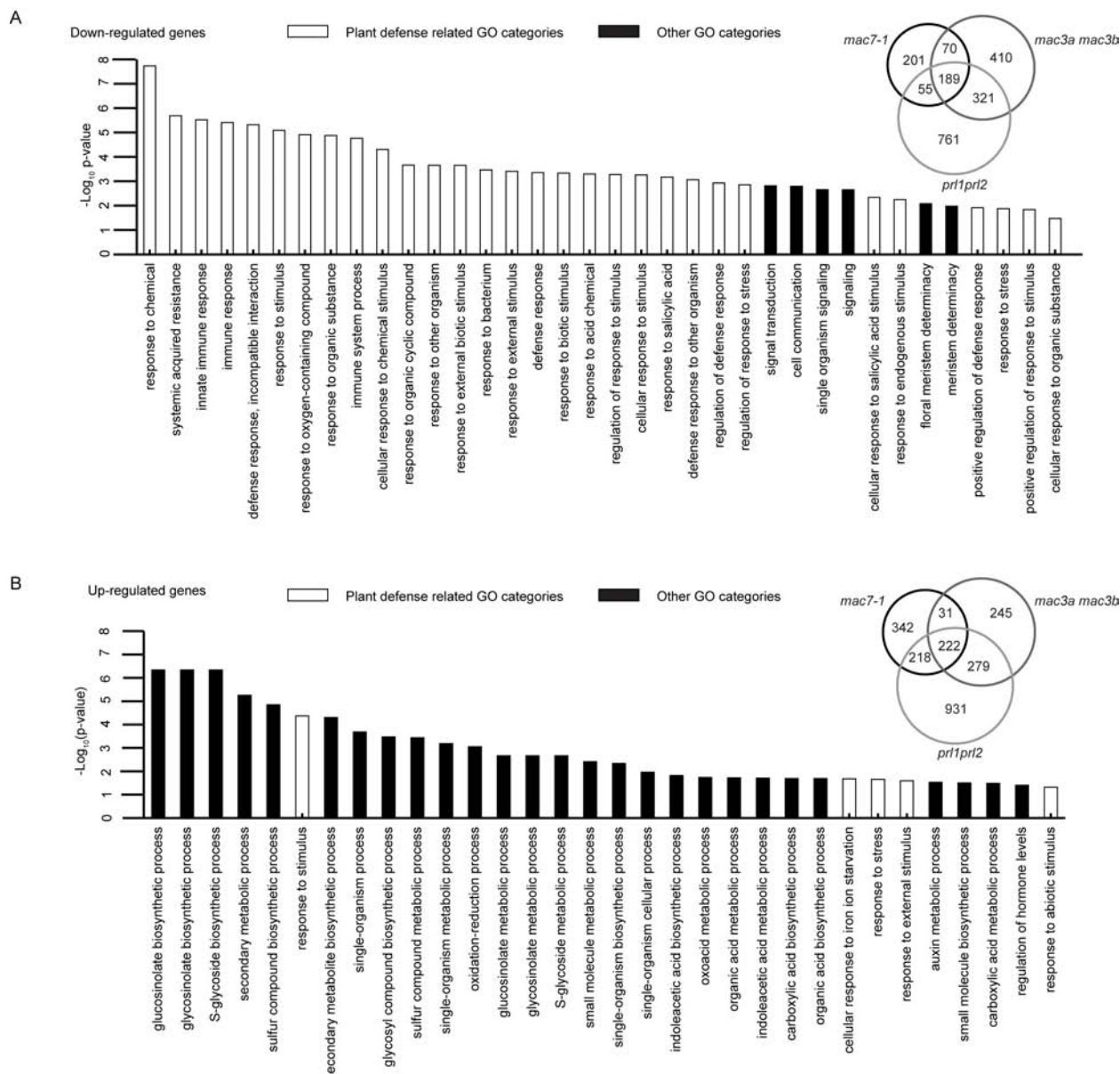


Figure 7. Down-regulated genes in the *mac* mutants are significantly related to stress responses, while up-regulated genes are involved in various biosynthetic and metabolic processes.

(A) GO enrichment analysis of 189 commonly down-regulated genes in *mac7-1*, *mac3a mac3b* and *prl1 prl2*. The degree of overlap among down-regulated genes in *mac7-1*, *mac3a mac3b* and *prl1 prl2* is shown in the Venn diagram. (B) GO enrichment analysis of 222 commonly up-regulated genes *mac7-1*, *mac3a mac3b* and *prl1 prl2*. The degree of overlap among up-regulated genes in *mac7-1*, *mac3a mac3b* and *prl1 prl2* is shown in the Venn diagram.

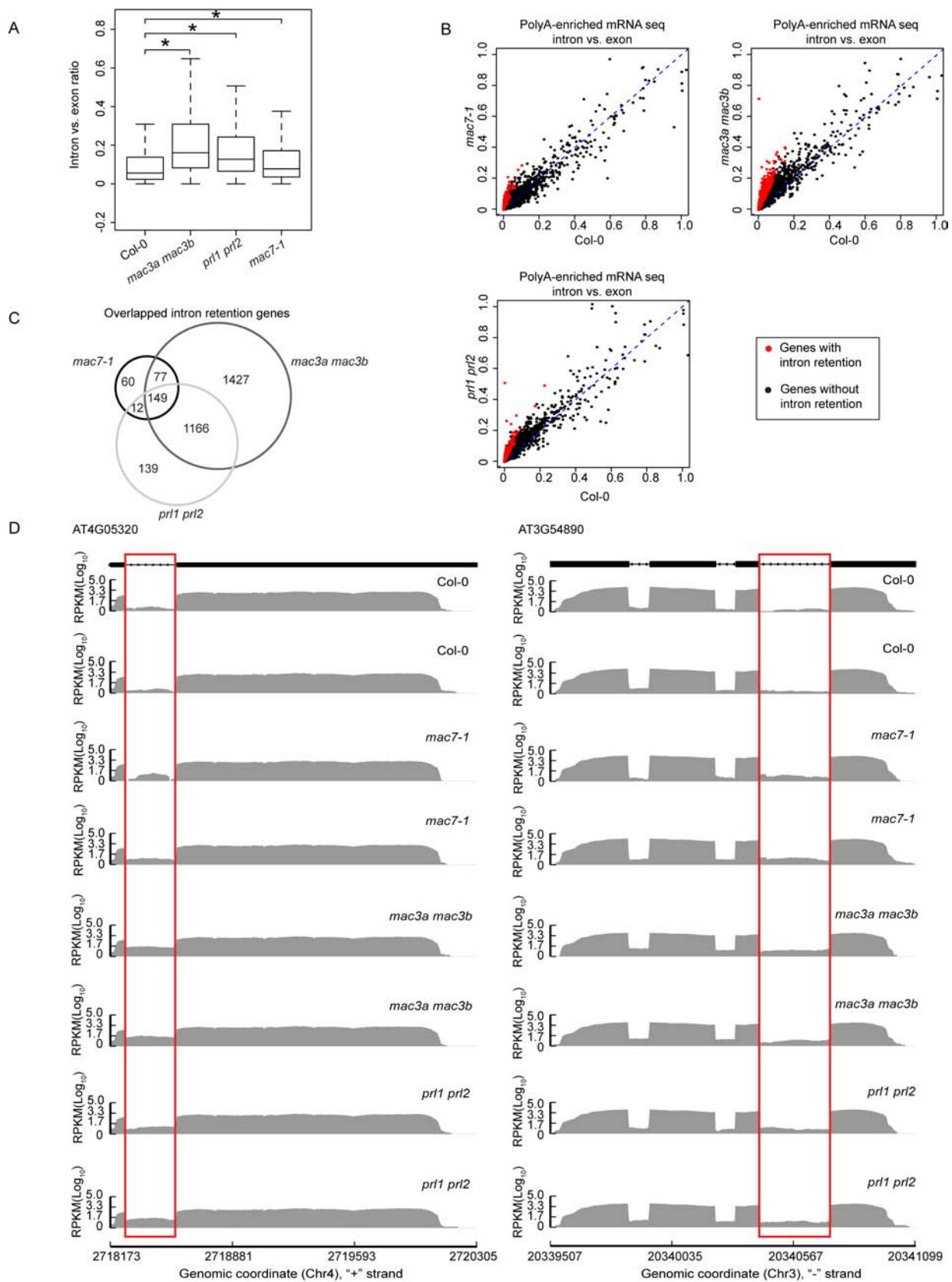


Figure 8. MAC subunits affect pre-mRNA splicing.

(A) Box plot of intron/exon ratios in the indicated genotypes. All genes that pass an abundance filter in expression were included in this analysis. Asterisks indicate significant difference between the mutant and wild type (Col-0) (Wilcoxon test, $p < 2.2\text{e-}16$). (B) The intron/exon ratio per gene in Col-0 vs. the indicated mutants. Black dots represent all genes with raw intronic read number ≥ 2 , exonic read number ≥ 5 , and final intron/exon ratio between 0 to 1. Red dots represent genes with significantly higher intron/exon ratio relative to wild type (fold change ≥ 2 and FDR < 0.01). (C) A Venn diagram showing the degree of overlap among genes with intron retention defects in *mac7-1*, *mac3a* *mac3b* and *prl1* *prl2*. (D) Examples of genes with intron retention defects. RPKM: Reads Per Kilobase per Million mapped reads. Two biological replicates for each genotype are shown. The rectangles mark introns with higher retention in the mutants.

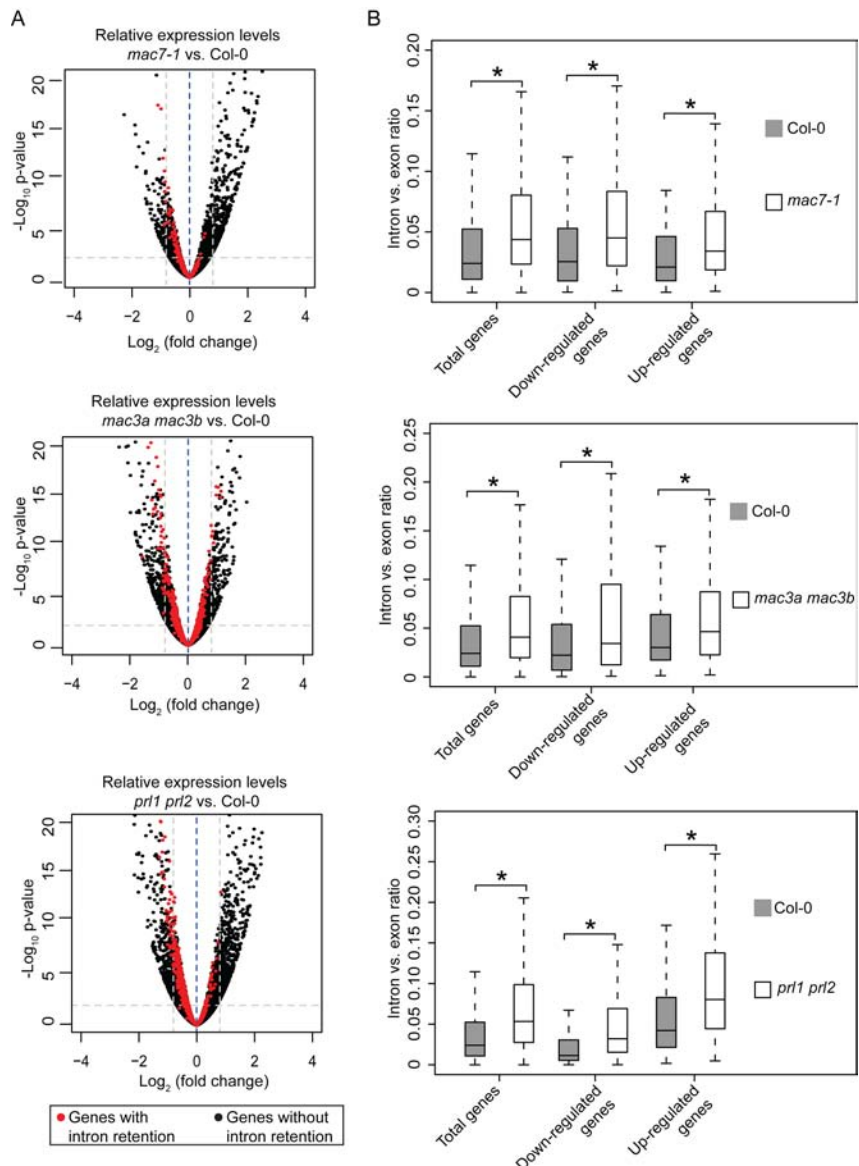


Figure 9. MAC affects pre-mRNA splicing and gene expression independently.

(A) Volcano plots illustrating fold changes of gene expression levels in the indicated mutants compared to Col-0. Thresholds for fold change of 1.5 and $p \leq 0.01$ are shown in the plots as gray dashed lines. Black dots and red dots represent the same genes as in Figure 8B. (B) Box plots of intron/exon ratios in total genes, up-regulated and down-regulated genes in the indicated genotypes. Only genes that pass an abundance filter (raw intronic read number ≥ 2 and exonic read number ≥ 5) were included in this analysis. Asterisks indicate significant difference between the mutant and wild type (Col-0) (Wilcoxon test, $p < 2.2e-16$).

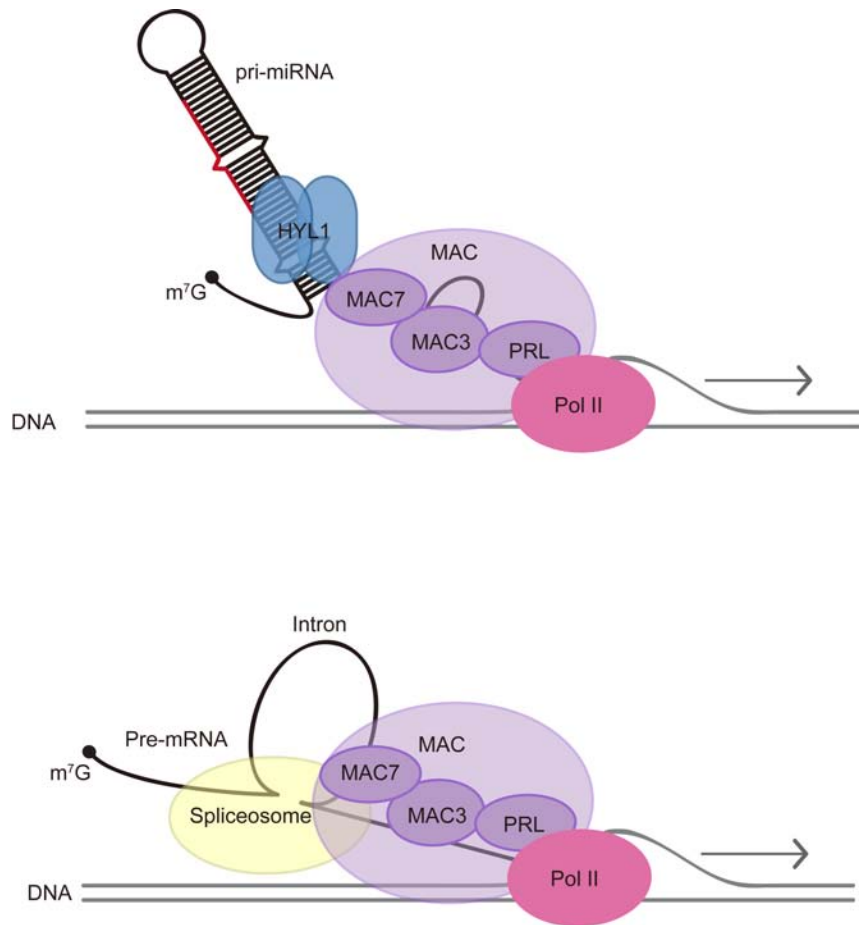


Figure 10. A model for MAC's functions in miRNA biogenesis and pre-mRNA processing.
 MAC affects miRNA biogenesis through influencing Pol II transcription and interacting with the pri-miRNA processing factor HYL1. MAC also plays a role in pre-mRNA splicing through interactions with the spliceosome. MAC seems to have separate roles in miRNA biogenesis and RNA splicing but a common theme appears to be co-transcriptional RNA processing.

Parsed Citations

Achkar, N.P., Cambiagno, D.A., and Manavella, P.A. (2016). miRNA Biogenesis: A Dynamic Pathway. *Trends Plant Sci.* 21, 1034-1044.

Pubmed: [Author and Title](#)

CrossRef: [Author and Title](#)

Google Scholar: [Author Only Title Only Author and Title](#)

Akay, A., Di Domenico, T., Suen, K.M., Nabih, A., Parada, G.E., Larance, M., Medhi, R., Berk'yurek, A.C., Zhang, X., Wedeles, C.J., Rudolph, K.L.M., Engelhardt, J., Hemberg, M., Ma, P., Lamond, A.I., Claycomb, J.M., and Miska, E.A. (2017). The Helicase Aquarius/EMB-4 Is Required to Overcome Intronic Barriers to Allow Nuclear RNAi Pathways to Heritably Silence Transcription. *Dev. Cell* 42, 241-255 e246.

Pubmed: [Author and Title](#)

CrossRef: [Author and Title](#)

Google Scholar: [Author Only Title Only Author and Title](#)

Arribas-Hernandez, L., Marchais, A., Poulsen, C., Haase, B., Hauptmann, J., Benes, V., Meister, G., and Brodersen, P. (2016). The Slicer Activity of ARGONAUTE1 Is Required Specifically for the Phasing, Not Production, of Trans-Acting Short Interfering RNAs in Arabidopsis. *Plant Cell* 28, 1563-1580.

Pubmed: [Author and Title](#)

CrossRef: [Author and Title](#)

Google Scholar: [Author Only Title Only Author and Title](#)

Baumberger, N., and Baulcombe, D.C. (2005). Arabidopsis ARGONAUTE1 is an RNA Slicer that selectively recruits microRNAs and short interfering RNAs. *Proc Natl Acad Sci U S A* 102, 11928-11933.

Pubmed: [Author and Title](#)

CrossRef: [Author and Title](#)

Google Scholar: [Author Only Title Only Author and Title](#)

Carbonell, A., Fahlgren, N., Garcia-Ruiz, H., Gilbert, K.B., Montgomery, T.A., Nguyen, T., Cuperus, J.T., and Carrington, J.C. (2012). Functional analysis of three Arabidopsis ARGONAUTES using slicer-defective mutants. *Plant Cell* 24, 3613-3629.

Pubmed: [Author and Title](#)

CrossRef: [Author and Title](#)

Google Scholar: [Author Only Title Only Author and Title](#)

Chanarat, S., and Strasser, K. (2013). Splicing and beyond: the many faces of the Prp19 complex. *Biochim. Biophys. Acta* 1833, 2126-2134.

Pubmed: [Author and Title](#)

CrossRef: [Author and Title](#)

Google Scholar: [Author Only Title Only Author and Title](#)

Chanarat, S., Seizl, M., and Strasser, K. (2011). The Prp19 complex is a novel transcription elongation factor required for TREX occupancy at transcribed genes. *Genes Dev.* 25, 1147-1158.

Pubmed: [Author and Title](#)

CrossRef: [Author and Title](#)

Google Scholar: [Author Only Title Only Author and Title](#)

Chanarat, S., Burkert-Kautzsch, C., Meinel, D.M., and Strasser, K. (2012). Prp19C and TREX: interacting to promote transcription elongation and mRNA export. *Transcription* 3, 8-12.

Pubmed: [Author and Title](#)

CrossRef: [Author and Title](#)

Google Scholar: [Author Only Title Only Author and Title](#)

Chicchi, P.M., and Kelly, W.G. (2006). emb-4 is a conserved gene required for efficient germline-specific chromatin remodeling during *Caenorhabditis elegans* embryogenesis. *Genetics* 174, 1895-1906.

Pubmed: [Author and Title](#)

CrossRef: [Author and Title](#)

Google Scholar: [Author Only Title Only Author and Title](#)

Curtis, M.D., and Grossniklaus, U. (2003). A gateway cloning vector set for high-throughput functional analysis of genes in planta. *Plant Physiol.* 133, 462-469.

Pubmed: [Author and Title](#)

CrossRef: [Author and Title](#)

Google Scholar: [Author Only Title Only Author and Title](#)

de Felippe, F.F., Ott, F., and Weigel, D. (2011). Comparative analysis of non-autonomous effects of tasiRNAs and miRNAs in *Arabidopsis thaliana*. *Nucleic Acids Res.* 39, 2880-2889.

Pubmed: [Author and Title](#)

CrossRef: [Author and Title](#)

Google Scholar: [Author Only Title Only Author and Title](#)

De, I., Bessonov, S., Hofele, R., dos Santos, K., Will, C.L., Urlaub, H., Luhrmann, R., and Pena, V. (2015). The RNA helicase Aquarius exhibits structural adaptations mediating its recruitment to spliceosomes. *Nat. Struct. Mol. Biol.* 22, 138-144.

Pubmed: [Author and Title](#)

CrossRef: [Author and Title](#)

Google Scholar: [Author Only](#) [Title Only](#) [Author and Title](#)

Deng, X., Lu, T., Wang, L., Gu, L., Sun, J., Kong, X., Liu, C., and Cao, X. (2016). Recruitment of the NineTeen Complex to the activated spliceosome requires AtPRMT5. *Proc Natl Acad Sci U S A* 113, 5447-5452.

Pubmed: [Author and Title](#)

CrossRef: [Author and Title](#)

Google Scholar: [Author Only](#) [Title Only](#) [Author and Title](#)

Dong, Z., Han, M.H., and Fedoroff, N. (2008). The RNA-binding proteins HYL1 and SE promote accurate in vitro processing of pri-miRNA by DCL1. *Proc Natl Acad Sci U S A* 105, 9970-9975.

Pubmed: [Author and Title](#)

CrossRef: [Author and Title](#)

Google Scholar: [Author Only](#) [Title Only](#) [Author and Title](#)

Earley, K.W., Haag, J.R., Pontes, O., Opper, K., Juehne, T., Song, K., and Pikaard, C.S. (2006). Gateway-compatible vectors for plant functional genomics and proteomics. *Plant J.* 45, 616-629.

Pubmed: [Author and Title](#)

CrossRef: [Author and Title](#)

Google Scholar: [Author Only](#) [Title Only](#) [Author and Title](#)

Edgar, R.C. (2004). MUSCLE: multiple sequence alignment with high accuracy and high throughput. *Nucleic Acids Res.* 32, 1792-1797.

Pubmed: [Author and Title](#)

CrossRef: [Author and Title](#)

Google Scholar: [Author Only](#) [Title Only](#) [Author and Title](#)

Fang, X., Cui, Y., Li, Y., and Qi, Y. (2015). Transcription and processing of primary microRNAs are coupled by Elongator complex in *Arabidopsis*. *Nat Plants* 1, 15075.

Pubmed: [Author and Title](#)

CrossRef: [Author and Title](#)

Google Scholar: [Author Only](#) [Title Only](#) [Author and Title](#)

Fang, Y., and Spector, D.L. (2007). Identification of nuclear dicing bodies containing proteins for microRNA biogenesis in living *Arabidopsis* plants. *Curr. Biol.* 17, 818-823.

Pubmed: [Author and Title](#)

CrossRef: [Author and Title](#)

Google Scholar: [Author Only](#) [Title Only](#) [Author and Title](#)

Francisco-Mangilet, A.G., Karlsson, P., Kim, M.H., Eo, H.J., Oh, S.A., Kim, J.H., Kulcheski, F.R., Park, S.K., and Manavella, P.A. (2015). THO2, a core member of the THO/TREX complex, is required for microRNA production in *Arabidopsis*. *Plant J.* 82, 1018-1029.

Pubmed: [Author and Title](#)

CrossRef: [Author and Title](#)

Google Scholar: [Author Only](#) [Title Only](#) [Author and Title](#)

Furumizu, C., Tsukaya, H., and Komeda, Y. (2010). Characterization of EMU, the *Arabidopsis* homolog of the yeast THO complex member HPR1. *RNA* 16, 1809-1817.

Pubmed: [Author and Title](#)

CrossRef: [Author and Title](#)

Google Scholar: [Author Only](#) [Title Only](#) [Author and Title](#)

Gene Ontology, C. (2015). Gene Ontology Consortium: going forward. *Nucleic Acids Res.* 43, D1049-1056.

Pubmed: [Author and Title](#)

CrossRef: [Author and Title](#)

Google Scholar: [Author Only](#) [Title Only](#) [Author and Title](#)

Hajheidari, M., Farrona, S., Huettel, B., Koncz, Z., and Koncz, C. (2012). CDKF1 and CDKD protein kinases regulate phosphorylation of serine residues in the C-terminal domain of *Arabidopsis* RNA polymerase II. *Plant Cell* 24, 1626-1642.

Pubmed: [Author and Title](#)

CrossRef: [Author and Title](#)

Google Scholar: [Author Only](#) [Title Only](#) [Author and Title](#)

Han, M.H., Goud, S., Song, L., and Fedoroff, N. (2004). The *Arabidopsis* double-stranded RNA-binding protein HYL1 plays a role in microRNA-mediated gene regulation. *Proc Natl Acad Sci U S A* 101, 1093-1098.

Pubmed: [Author and Title](#)

CrossRef: [Author and Title](#)

Google Scholar: [Author Only](#) [Title Only](#) [Author and Title](#)

Hirose, T., Ideue, T., Nagai, M., Hagiwara, M., Shu, M.D., and Steitz, J.A. (2006). A spliceosomal intron binding protein, IBP160, links position-dependent assembly of intron-encoded box C/D snoRNP to pre-mRNA splicing. *Mol. Cell* 23, 673-684.

Pubmed: [Author and Title](#)

CrossRef: [Author and Title](#)

Google Scholar: [Author Only](#) [Title Only](#) [Author and Title](#)

Ji, L., Liu, X., Yan, J., Wang, W., Yumul, R.E., Kim, Y.J., Dinh, T.T., Liu, J., Cui, X., Zheng, B., Agarwal, M., Liu, C., Cao, X., Tang, G., and Chen, X. (2011). ARGONAUTE10 and ARGONAUTE1 regulate the termination of floral stem cells through two microRNAs in *Arabidopsis*. *PLoS Genet.* 7, e1001358.

Pubmed: [Author and Title](#)

CrossRef: [Author and Title](#)

Google Scholar: [Author Only Title Only Author and Title](#)

Johnson, K.C.M., Dong, O.X., and Li, X. (2011). The evolutionarily conserved MOS4-associated complex. Central European Journal of Biology 6, 776-784.

Pubmed: [Author and Title](#)

CrossRef: [Author and Title](#)

Google Scholar: [Author Only Title Only Author and Title](#)

Johnson, N.R., Yeoh, J.M., Coruh, C., and Axtell, M.J. (2016). Improved Placement of Multi-mapping Small RNAs. G3 (Bethesda) 6, 2103-2111.

Pubmed: [Author and Title](#)

CrossRef: [Author and Title](#)

Google Scholar: [Author Only Title Only Author and Title](#)

Karlsson, P., Christie, M.D., Seymour, D.K., Wang, H., Wang, X., Hagmann, J., Kulcheski, F., and Manavella, P.A. (2015). KH domain protein RCF3 is a tissue-biased regulator of the plant miRNA biogenesis cofactor HYL1. Proc Natl Acad Sci U S A 112, 14096-14101.

Pubmed: [Author and Title](#)

CrossRef: [Author and Title](#)

Google Scholar: [Author Only Title Only Author and Title](#)

Kim, D., Langmead, B., and Salzberg, S.L. (2015). HISAT: a fast spliced aligner with low memory requirements. Nat. Methods 12, 357-360.

Pubmed: [Author and Title](#)

CrossRef: [Author and Title](#)

Google Scholar: [Author Only Title Only Author and Title](#)

Kim, Y.J., Zheng, B., Yu, Y., Won, S.Y., Mo, B., and Chen, X. (2011). The role of Mediator in small and long noncoding RNA production in *Arabidopsis thaliana*. EMBO J. 30, 814-822.

Pubmed: [Author and Title](#)

CrossRef: [Author and Title](#)

Google Scholar: [Author Only Title Only Author and Title](#)

Koncz, C., Dejong, F., Villacorta, N., Szakonyi, D., and Koncz, Z. (2012). The spliceosome-activating complex: molecular mechanisms underlying the function of a pleiotropic regulator. Front Plant Sci 3, 9.

Pubmed: [Author and Title](#)

CrossRef: [Author and Title](#)

Google Scholar: [Author Only Title Only Author and Title](#)

Kuraoka, I., Ito, S., Wada, T., Hayashida, M., Lee, L., Saito, M., Nakatsu, Y., Matsumoto, M., Matsunaga, T., Handa, H., Qin, J., Nakatani, Y., and Tanaka, K. (2008). Isolation of XAB2 complex involved in pre-mRNA splicing, transcription, and transcription-coupled repair. J. Biol. Chem. 283, 940-950.

Pubmed: [Author and Title](#)

CrossRef: [Author and Title](#)

Google Scholar: [Author Only Title Only Author and Title](#)

Kurihara, Y., and Watanabe, Y. (2004). Arabidopsis micro-RNA biogenesis through Dicer-like 1 protein functions. Proc Natl Acad Sci U S A 101, 12753-12758.

Pubmed: [Author and Title](#)

CrossRef: [Author and Title](#)

Google Scholar: [Author Only Title Only Author and Title](#)

Kurihara, Y., Takashi, Y., and Watanabe, Y. (2006). The interaction between DCL1 and HYL1 is important for efficient and precise processing of pri-miRNA in plant microRNA biogenesis. RNA 12, 206-212.

Pubmed: [Author and Title](#)

CrossRef: [Author and Title](#)

Google Scholar: [Author Only Title Only Author and Title](#)

Laubinger, S., Sachsenberg, T., Zeller, G., Busch, W., Lohmann, J.U., Ratsch, G., and Weigel, D. (2008). Dual roles of the nuclear cap-binding complex and SERRATE in pre-mRNA splicing and microRNA processing in *Arabidopsis thaliana*. Proc Natl Acad Sci U S A 105, 8795-8800.

Pubmed: [Author and Title](#)

CrossRef: [Author and Title](#)

Google Scholar: [Author Only Title Only Author and Title](#)

Li, H., and Durbin, R. (2009). Fast and accurate short read alignment with Burrows-Wheeler transform. Bioinformatics 25, 1754-1760.

Pubmed: [Author and Title](#)

CrossRef: [Author and Title](#)

Google Scholar: [Author Only Title Only Author and Title](#)

Li, H., Ruan, J., and Durbin, R. (2008). Mapping short DNA sequencing reads and calling variants using mapping quality scores. Genome Res. 18, 1851-1858.

Pubmed: [Author and Title](#)

CrossRef: [Author and Title](#)

Google Scholar: [Author Only Title Only Author and Title](#)

Li, H., Handsaker, B., Wysoker, A., Fennell, T., Ruan, J., Homer, N., Marth, G., Abecasis, G., Durbin, R., and Genome Project Data Processing, S. (2009). The Sequence Alignment/Map format and SAMtools. *Bioinformatics* 25, 2078-2079.

Pubmed: [Author and Title](#)

CrossRef: [Author and Title](#)

Google Scholar: [Author Only Title Only Author and Title](#)

Li, J., Yang, Z., Yu, B., Liu, J., and Chen, X. (2005). Methylation protects miRNAs and siRNAs from a 3'-end uridylation activity in *Arabidopsis*. *Curr. Biol.* 15, 1501-1507.

Pubmed: [Author and Title](#)

CrossRef: [Author and Title](#)

Google Scholar: [Author Only Title Only Author and Title](#)

Li, S., Le, B., Ma, X., Li, S., You, C., Yu, Y., Zhang, B., Liu, L., Gao, L., Shi, T., Zhao, Y., Mo, B., Cao, X., and Chen, X. (2016). Biogenesis of phased siRNAs on membrane-bound polysomes in *Arabidopsis*. *Elife* 5.

Pubmed: [Author and Title](#)

CrossRef: [Author and Title](#)

Google Scholar: [Author Only Title Only Author and Title](#)

Lidder, P., Gutierrez, R.A., Salome, P.A., McClung, C.R., and Green, P.J. (2005). Circadian control of messenger RNA stability. Association with a sequence-specific messenger RNA decay pathway. *Plant Physiol.* 138, 2374-2385.

Pubmed: [Author and Title](#)

CrossRef: [Author and Title](#)

Google Scholar: [Author Only Title Only Author and Title](#)

Lin, Z., Yin, K., Zhu, D., Chen, Z., Gu, H., and Qu, L.J. (2007). AtCDC5 regulates the G2 to M transition of the cell cycle and is critical for the function of *Arabidopsis* shoot apical meristem. *Cell Res.* 17, 815-828.

Pubmed: [Author and Title](#)

CrossRef: [Author and Title](#)

Google Scholar: [Author Only Title Only Author and Title](#)

Love, M.I., Huber, W., and Anders, S. (2014). Moderated estimation of fold change and dispersion for RNA-seq data with DESeq2. *Genome Biol* 15, 550.

Pubmed: [Author and Title](#)

CrossRef: [Author and Title](#)

Google Scholar: [Author Only Title Only Author and Title](#)

Manavella, P.A., Hagmann, J., Ott, F., Laubinger, S., Franz, M., Macek, B., and Weigel, D. (2012). Fast-forward genetics identifies plant CPL phosphatases as regulators of miRNA processing factor HYL1. *Cell* 151, 859-870.

Pubmed: [Author and Title](#)

CrossRef: [Author and Title](#)

Google Scholar: [Author Only Title Only Author and Title](#)

Martin, M. (2011). Cutadapt removes adapter sequences from high-throughput sequencing reads. *EMBnet.journal* 17, 10-12.

Pubmed: [Author and Title](#)

CrossRef: [Author and Title](#)

Google Scholar: [Author Only Title Only Author and Title](#)

Monaghan, J., Xu, F., Xu, S., Zhang, Y., and Li, X. (2010). Two putative RNA-binding proteins function with unequal genetic redundancy in the MOS4-associated complex. *Plant Physiol.* 154, 1783-1793.

Pubmed: [Author and Title](#)

CrossRef: [Author and Title](#)

Google Scholar: [Author Only Title Only Author and Title](#)

Monaghan, J., Xu, F., Gao, M., Zhao, Q., Palma, K., Long, C., Chen, S., Zhang, Y., and Li, X. (2009). Two Prp19-like U-box proteins in the MOS4-associated complex play redundant roles in plant innate immunity. *PLoS Pathog* 5, e1000526.

Pubmed: [Author and Title](#)

CrossRef: [Author and Title](#)

Google Scholar: [Author Only Title Only Author and Title](#)

Nakamura, S., Mano, S., Tanaka, Y., Ohnishi, M., Nakamori, C., Araki, M., Niwa, T., Nishimura, M., Kaminaka, H., Nakagawa, T., Sato, Y., and Ishiguro, S. (2010). Gateway binary vectors with the bialaphos resistance gene, bar, as a selection marker for plant transformation. *Biosci Biotechnol Biochem* 74, 1315-1319.

Pubmed: [Author and Title](#)

CrossRef: [Author and Title](#)

Google Scholar: [Author Only Title Only Author and Title](#)

Nemeth, K., Salchert, K., Putnoky, P., Bhalerao, R., Koncz-Kalman, Z., Stankovic-Stangeland, B., Bako, L., Mathur, J., Okresz, L., Stabel, S., Geigenberger, P., Stitt, M., Redei, G.P., Schell, J., and Koncz, C. (1998). Pleiotropic control of glucose and hormone responses by PRL1, a nuclear WD protein, in *Arabidopsis*. *Genes Dev.* 12, 3059-3073.

Pubmed: [Author and Title](#)

CrossRef: [Author and Title](#)

Google Scholar: [Author Only Title Only Author and Title](#)

Ner-Gaon, H., Halachmi, R., Savaldi-Goldstein, S., Rubin, E., Ophir, R., and Fluhr, R. (2004). Intron retention is a major phenomenon in alternative splicing in *Arabidopsis*. *Plant J.* 39, 877-885.

Pubmed: [Author and Title](#)

CrossRef: [Author and Title](#)

Google Scholar: [Author Only Title Only Author and Title](#)

Ozgur, S., Buchwald, G., Falk, S., Chakrabarti, S., Prabu, J.R., and Conti, E. (2015). The conformational plasticity of eukaryotic RNA-dependent ATPases. FEBS J. 282, 850-863.

Pubmed: [Author and Title](#)

CrossRef: [Author and Title](#)

Google Scholar: [Author Only Title Only Author and Title](#)

Pall, G.S., and Hamilton, A.J. (2008). Improved northern blot method for enhanced detection of small RNA. Nat Protoc 3, 1077-1084.

Pubmed: [Author and Title](#)

CrossRef: [Author and Title](#)

Google Scholar: [Author Only Title Only Author and Title](#)

Palma, K., Zhao, Q., Cheng, Y.T., Bi, D., Monaghan, J., Cheng, W., Zhang, Y., and Li, X. (2007). Regulation of plant innate immunity by three proteins in a complex conserved across the plant and animal kingdoms. Genes Dev. 21, 1484-1493.

Pubmed: [Author and Title](#)

CrossRef: [Author and Title](#)

Google Scholar: [Author Only Title Only Author and Title](#)

Park, W., Li, J., Song, R., Messing, J., and Chen, X. (2002). CARPEL FACTORY, a Dicer homolog, and HEN1, a novel protein, act in microRNA metabolism in *Arabidopsis thaliana*. Curr. Biol. 12, 1484-1495.

Pubmed: [Author and Title](#)

CrossRef: [Author and Title](#)

Google Scholar: [Author Only Title Only Author and Title](#)

Peterson, R., Slovin, J.P., and Chen, C. (2010). A simplified method for differential staining of aborted and non-aborted pollen grains. Int J Plant Biol 1:e13, 66-69.

Pubmed: [Author and Title](#)

CrossRef: [Author and Title](#)

Google Scholar: [Author Only Title Only Author and Title](#)

Qiao, Y., Shi, J., Zhai, Y., Hou, Y., and Ma, W. (2015). Phytophthora effector targets a novel component of small RNA pathway in plants to promote infection. Proc Natl Acad Sci U S A 112, 5850-5855.

Pubmed: [Author and Title](#)

CrossRef: [Author and Title](#)

Google Scholar: [Author Only Title Only Author and Title](#)

Raczynska, K.D., Stepien, A., Kierzkowski, D., Kalak, M., Bajczyk, M., McNicol, J., Simpson, C.G., Szweykowska-Kulinska, Z., Brown, J.W., and Jarmolowski, A. (2014). The SERRATE protein is involved in alternative splicing in *Arabidopsis thaliana*. Nucleic Acids Res. 42, 1224-1244.

Pubmed: [Author and Title](#)

CrossRef: [Author and Title](#)

Google Scholar: [Author Only Title Only Author and Title](#)

Ren, G., Xie, M., Dou, Y., Zhang, S., Zhang, C., and Yu, B. (2012). Regulation of miRNA abundance by RNA binding protein TOUGH in *Arabidopsis*. Proc Natl Acad Sci U S A 109, 12817-12821.

Pubmed: [Author and Title](#)

CrossRef: [Author and Title](#)

Google Scholar: [Author Only Title Only Author and Title](#)

Rogers, K., and Chen, X. (2013). Biogenesis, turnover, and mode of action of plant microRNAs. Plant Cell 25, 2383-2399.

Pubmed: [Author and Title](#)

CrossRef: [Author and Title](#)

Google Scholar: [Author Only Title Only Author and Title](#)

Sleat, D.E., Zheng, H., Qian, M., and Lobel, P. (2006). Identification of sites of mannose 6-phosphorylation on lysosomal proteins. Mol. Cell. Proteomics 5, 686-701.

Pubmed: [Author and Title](#)

CrossRef: [Author and Title](#)

Google Scholar: [Author Only Title Only Author and Title](#)

Song, L., Han, M.H., Lesicka, J., and Fedoroff, N. (2007). Arabidopsis primary microRNA processing proteins HYL1 and DCL1 define a nuclear body distinct from the Cajal body. Proc Natl Acad Sci U S A 104, 5437-5442.

Pubmed: [Author and Title](#)

CrossRef: [Author and Title](#)

Google Scholar: [Author Only Title Only Author and Title](#)

Sparks, I.A., Runions, J., Kearns, A., and Hawes, C. (2006). Rapid, transient expression of fluorescent fusion proteins in tobacco plants and generation of stably transformed plants. Nat Protoc 1, 2019-2025.

Pubmed: [Author and Title](#)

CrossRef: [Author and Title](#)

Google Scholar: [Author Only Title Only Author and Title](#)

Szarzynska, B., Sobkowiak, L., Pant, B.D., Balazadeh, S., Scheible, W.R., Mueller-Roeber, B., Jarmolowski, A., and Szweykowska-

Kulinska, Z (2009). Gene structures and processing of *Arabidopsis thaliana* HYL1-dependent pri-miRNAs. *Nucleic Acids Res.* 37, 3083-3093.

Pubmed: [Author and Title](#)

CrossRef: [Author and Title](#)

Google Scholar: [Author Only Title Only Author and Title](#)

Tyc, K.M., Nabih, A., Wu, M.Z., Wedeles, C.J., Sobotka, J.A., and Claycomb, J.M. (2017). The Conserved Intron Binding Protein EMB-4 Plays Differential Roles in Germline Small RNA Pathways of *C. elegans*. *Dev. Cell* 42, 256-270 e256.

Pubmed: [Author and Title](#)

CrossRef: [Author and Title](#)

Google Scholar: [Author Only Title Only Author and Title](#)

Tzafrir, I., Pena-Muralla, R., Dickerman, A., Berg, M., Rogers, R., Hutchens, S., Sweeney, T.C., McElver, J., Aux, G., Patton, D., and Meinke, D. (2004). Identification of genes required for embryo development in *Arabidopsis*. *Plant Physiol.* 135, 1206-1220.

Pubmed: [Author and Title](#)

CrossRef: [Author and Title](#)

Google Scholar: [Author Only Title Only Author and Title](#)

Walter, M., Chaban, C., Schutze, K., Batistic, O., Weckermann, K., Nake, C., Blazevic, D., Grefen, C., Schumacher, K., Oecking, C., Harter, K., and Kudla, J. (2004). Visualization of protein interactions in living plant cells using bimolecular fluorescence complementation. *Plant J.* 40, 428-438.

Pubmed: [Author and Title](#)

CrossRef: [Author and Title](#)

Google Scholar: [Author Only Title Only Author and Title](#)

Wang, L., Song, X., Gu, L., Li, X., Cao, S., Chu, C., Cui, X., Chen, X., and Cao, X. (2013). NOT2 proteins promote polymerase II-dependent transcription and interact with multiple MicroRNA biogenesis factors in *Arabidopsis*. *Plant Cell* 25, 715-727.

Pubmed: [Author and Title](#)

CrossRef: [Author and Title](#)

Google Scholar: [Author Only Title Only Author and Title](#)

Wang, M., Zhao, Y., and Zhang, B. (2015). Efficient Test and Visualization of Multi-Set Intersections. *Sci Rep* 5, 16923.

Pubmed: [Author and Title](#)

CrossRef: [Author and Title](#)

Google Scholar: [Author Only Title Only Author and Title](#)

Waterhouse, A.M., Procter, J.B., Martin, D.M., Clamp, M., and Barton, G.J. (2009). Jalview Version 2—a multiple sequence alignment editor and analysis workbench. *Bioinformatics* 25, 1189-1191.

Pubmed: [Author and Title](#)

CrossRef: [Author and Title](#)

Google Scholar: [Author Only Title Only Author and Title](#)

Weihmann, T., Palma, K., Nitta, Y., and Li, X. (2012). Pleiotropic regulatory locus 2 exhibits unequal genetic redundancy with its homolog PRL1. *Plant Cell Physiol.* 53, 1617-1626.

Pubmed: [Author and Title](#)

CrossRef: [Author and Title](#)

Google Scholar: [Author Only Title Only Author and Title](#)

Wiborg, J., O'Shea, C., and Skriver, K. (2008). Biochemical function of typical and variant *Arabidopsis thaliana* U-box E3 ubiquitin-protein ligases. *Biochem. J.* 413, 447-457.

Pubmed: [Author and Title](#)

CrossRef: [Author and Title](#)

Google Scholar: [Author Only Title Only Author and Title](#)

Wu, X., Shi, Y., Li, J., Xu, L., Fang, Y., Li, X., and Qi, Y. (2013). A role for the RNA-binding protein MOS2 in microRNA maturation in *Arabidopsis*. *Cell Res.* 23, 645-657.

Pubmed: [Author and Title](#)

CrossRef: [Author and Title](#)

Google Scholar: [Author Only Title Only Author and Title](#)

Xie, Z., Allen, E., Fahlgren, N., Calamar, A., Givan, S.A., and Carrington, J.C. (2005). Expression of *Arabidopsis* MIRNA genes. *Plant Physiol.* 138, 2145-2154.

Pubmed: [Author and Title](#)

CrossRef: [Author and Title](#)

Google Scholar: [Author Only Title Only Author and Title](#)

Xu, F., Xu, S., Wiermer, M., Zhang, Y., and Li, X. (2012). The cyclin L homolog MOS12 and the MOS4-associated complex are required for the proper splicing of plant resistance genes. *Plant J.* 70, 916-928.

Pubmed: [Author and Title](#)

CrossRef: [Author and Title](#)

Google Scholar: [Author Only Title Only Author and Title](#)

Yan, C., Hang, J., Wan, R., Huang, M., Wong, C.C., and Shi, Y. (2015). Structure of a yeast spliceosome at 3.6-angstrom resolution. *Science* 349, 1182-1191.

Pubmed: [Author and Title](#)

CrossRef: [Author and Title](#)

Google Scholar: [Author Only Title Only Author and Title](#)

Yang, L., Liu, Z., Lu, F., Dong, A., and Huang, H. (2006a). SERRATE is a novel nuclear regulator in primary microRNA processing in Arabidopsis. *Plant J.* 47, 841-850.

Pubmed: [Author and Title](#)

CrossRef: [Author and Title](#)

Google Scholar: [Author Only Title Only Author and Title](#)

Yang, Z., Ebright, Y.W., Yu, B., and Chen, X. (2006b). HEN1 recognizes 21-24 nt small RNA duplexes and deposits a methyl group onto the 2' OH of the 3' terminal nucleotide. *Nucleic Acids Res.* 34, 667-675.

Pubmed: [Author and Title](#)

CrossRef: [Author and Title](#)

Google Scholar: [Author Only Title Only Author and Title](#)

Yu, B., Yang, Z., Li, J., Minakhina, S., Yang, M., Padgett, R.W., Steward, R., and Chen, X. (2005). Methylation as a crucial step in plant microRNA biogenesis. *Science* 307, 932-935.

Pubmed: [Author and Title](#)

CrossRef: [Author and Title](#)

Google Scholar: [Author Only Title Only Author and Title](#)

Yu, B., Bi, L., Zhai, J., Agarwal, M., Li, S., Wu, Q., Ding, S.W., Meyers, B.C., Vaucheret, H., and Chen, X. (2010). siRNAs compete with miRNAs for methylation by HEN1 in Arabidopsis. *Nucleic Acids Res.* 38, 5844-5850.

Pubmed: [Author and Title](#)

CrossRef: [Author and Title](#)

Google Scholar: [Author Only Title Only Author and Title](#)

Yu, B., Bi, L., Zheng, B., Ji, L., Chevalier, D., Agarwal, M., Ramachandran, V., Li, W., Lagrange, T., Walker, J.C., and Chen, X. (2008). The FHA domain proteins DAWdle in Arabidopsis and SNIP1 in humans act in small RNA biogenesis. *Proc Natl Acad Sci U S A* 105, 10073-10078.

Pubmed: [Author and Title](#)

CrossRef: [Author and Title](#)

Google Scholar: [Author Only Title Only Author and Title](#)

Zhan, X., Wang, B., Li, H., Liu, R., Kalia, R.K., Zhu, J.K., and Chinnusamy, V. (2012). Arabidopsis proline-rich protein important for development and abiotic stress tolerance is involved in microRNA biogenesis. *Proc Natl Acad Sci U S A* 109, 18198-18203.

Pubmed: [Author and Title](#)

CrossRef: [Author and Title](#)

Google Scholar: [Author Only Title Only Author and Title](#)

Zhang, C.J., Zhou, J.X., Liu, J., Ma, Z.Y., Zhang, S.W., Dou, K., Huang, H.W., Cai, T., Liu, R., Zhu, J.K., and He, X.J. (2013a). The splicing machinery promotes RNA-directed DNA methylation and transcriptional silencing in Arabidopsis. *EMBO J.* 32, 1128-1140.

Pubmed: [Author and Title](#)

CrossRef: [Author and Title](#)

Google Scholar: [Author Only Title Only Author and Title](#)

Zhang, S., Liu, Y., and Yu, B. (2014). PRL1, an RNA-binding protein, positively regulates the accumulation of miRNAs and siRNAs in Arabidopsis. *PLoS Genet.* 10, e1004841.

Pubmed: [Author and Title](#)

CrossRef: [Author and Title](#)

Google Scholar: [Author Only Title Only Author and Title](#)

Zhang, S., Xie, M., Ren, G., and Yu, B. (2013b). CDC5, a DNA binding protein, positively regulates posttranscriptional processing and/or transcription of primary microRNA transcripts. *Proc Natl Acad Sci U S A* 110, 17588-17593.

Pubmed: [Author and Title](#)

CrossRef: [Author and Title](#)

Google Scholar: [Author Only Title Only Author and Title](#)

Zheng, B., Wang, Z., Li, S., Yu, B., Liu, J.Y., and Chen, X. (2009). Intergenic transcription by RNA polymerase II coordinates Pol IV and Pol V in siRNA-directed transcriptional gene silencing in Arabidopsis. *Genes Dev.* 23, 2850-2860.

Pubmed: [Author and Title](#)

CrossRef: [Author and Title](#)

Google Scholar: [Author Only Title Only Author and Title](#)

Zielezinski, A., Dolata, J., Alaba, S., Kruszka, K., Pacak, A., Swida-Barteczka, A., Knop, K., Stepien, A., Bielewicz, D., Pietrykowska, H., Sierocka, I., Sobkowiak, L., Lakomia, A., Jarmolowski, A., Szweykowska-Kulinska, Z., and Karlowski, W.M. (2015). mirEX 2.0 - an integrated environment for expression profiling of plant microRNAs. *BMC Plant Biol.* 15, 144.

Pubmed: [Author and Title](#)

CrossRef: [Author and Title](#)

Google Scholar: [Author Only Title Only Author and Title](#)

**The Arabidopsis MOS4-associated Complex Promotes MicroRNA Biogenesis and Precursor
Messenger RNA Splicing**

Tianran Jia, Bailong Zhang, Chenjiang You, Yong Zhang, Liping Zeng, Shengjun li, Kaeli C.M. Johnson,

Bin Yu, Xin Li and Xuemei Chen

Plant Cell; originally published online September 25, 2017;

DOI 10.1105/tpc.17.00370

This information is current as of July 13, 2018

Supplemental Data

</content/suppl/2017/10/10/tpc.17.00370.DC1.html>
</content/suppl/2017/11/27/tpc.17.00370.DC2.html>
</content/suppl/2017/12/13/tpc.17.00370.DC3.html>

Permissions

https://www.copyright.com/ccc/openurl.do?sid=pd_hw1532298X&issn=1532298X&WT.mc_id=pd_hw1532298X

eTOCs

Sign up for eTOCs at:
<http://www.plantcell.org/cgi/alerts/ctmain>

CiteTrack Alerts

Sign up for CiteTrack Alerts at:
<http://www.plantcell.org/cgi/alerts/ctmain>

Subscription Information

Subscription Information for *The Plant Cell* and *Plant Physiology* is available at:
<http://www.aspb.org/publications/subscriptions.cfm>